

1

2 **Seasonal cycles and trends of water budget components in 18**  
3 **river basins across the Tibetan Plateau: a multiple datasets**  
4 **perspective**

5

6 Wenbin Liu<sup>a</sup>, Fubao Sun<sup>a\*</sup>, Yanzhong Li<sup>a</sup>, Guoqing Zhang<sup>b,c</sup>,

7 Yan-Fang Sang<sup>a</sup>, Jiahong Liu<sup>d</sup>, Hong Wang<sup>a</sup>, Peng Bai<sup>a</sup>

8

9 <sup>a</sup>Key Laboratory of Water Cycle and Related Land Surface Processes, Institute of Geographic  
10 Sciences and Natural Resources Research, Chinese Academy of Sciences, Beijing 100101, China

11 <sup>b</sup>Key Laboratory of Tibetan Environmental Changes and Land Surface Processes, Institute of  
12 Tibetan Plateau Research, Chinese Academy of Sciences, Beijing 100101, China

13 <sup>c</sup>CAS Center for Excellent in Tibetan Plateau Earth Sciences, Beijing 100101, China

14 <sup>d</sup>Key Laboratory of Simulation and Regulation of Water Cycle in River Basin, China Institute of  
15 Water Resources and Hydropower Research, Beijing 100038, China

16

17 **Submitted to:** Hydrology and Earth System Sciences

18 **Corresponding Author:** Dr. Fubao Sun ([Sunfb@igsnr.ac.cn](mailto:Sunfb@igsnr.ac.cn)), from the Key Laboratory of Water  
19 Cycle and Related Land Surface Processes, Institute of Geographic Sciences and Natural  
20 Resources Research, Chinese Academy of Sciences (No. A11, Datun Road, Chaoyang District,  
21 Beijing 100101, China)

22 **Email Addresses for other authors:** Wenbin Liu ([liuwb@igsnr.ac.cn](mailto:liuwb@igsnr.ac.cn)), Yanzhong Li  
23 ([liy.14b@igsnr.ac.cn](mailto:liy.14b@igsnr.ac.cn)), Guoqing Zhang ([guoqing.zhang@itpcas.ac.cn](mailto:guoqing.zhang@itpcas.ac.cn)), Yan-fang Sang  
24 ([sangyf@igsnr.ac.cn](mailto:sangyf@igsnr.ac.cn)), Jiahong Liu ([liujh@iwhr.com](mailto:liujh@iwhr.com)), Hong Wang ([wanghong@igsnr.ac.cn](mailto:wanghong@igsnr.ac.cn)),  
25 Peng Bai ([baip.11b@igsnr.ac.cn](mailto:baip.11b@igsnr.ac.cn))

26

27

2016/11/25

28

29 **Highlights**

- 30 ● Monthly basin-wide ET was calculated through water balance considering the  
31 impacts of glacier and water storage change
- 32 | ● Water budget components and trends for 18 river basins over the TP were  
33 evaluated
- 34 ● Uncertainties were discussed from multiple dataset perspective

35

36 | **Abstract.** The ~~insights dynamics~~ of water budget over ~~the~~ Tibetan Plateau (TP) are  
37 | not fully understood so far due to the lack of quantitative observations of the land  
38 | surface ~~processes water cycle~~. Here, we investigated the seasonal cycles and trends of  
39 | water budget components, ~~e.g., precipitation, runoff and evapotranspiration (ET)~~, in  
40 | 18 TP basins ~~through the use of using~~ multi-source datasets during the period  
41 | 1982-2011. A two-step bias correction procedure was applied to calculate the  
42 | basin-wide ~~evapotranspiration (ET) through the water balance~~ considering the  
43 | influences of glacier and water storage change. The results indicated that precipitation,  
44 | which mainly concentrated during June-October (varied among different monsoons  
45 | impacted basins), is the major contributor to the runoff in ~~the~~ TP basins. The  
46 | basin-wide snow water equivalent (SWE) was relatively higher from mid-autumn to  
47 | spring for most TP basins. The water cycles intensified under a global warming in  
48 | most basins except for the upper Yellow and Yalong Rivers, which were significantly  
49 | influenced by the weakening East Asian monsoon. ~~Corresponded to~~ Consistent with  
50 | the climate warming and moistening in the TP and western China, the aridity index  
51 | (PET/P) in most basins decreased. ~~The general hydrological regimes could be inferred~~  
52 | ~~from the perspective of multi-source datasets although there are considerable~~  
53 | ~~uncertainties from different datasets, which are comparable to some existing studies~~  
54 | ~~using the field observations and complex modeling approaches.~~ The results  
55 | highlighted the usefulness of integrating the multi-source data (e.g., in situ  
56 | observations, remote sensing products, reanalysis, land surface model simulations and  
57 | climate model outputs) for hydrological applications in the data-sparse ~~environments~~

58 | regions and could be ~~benefit-beneficial~~ for understanding the water and energy  
59 | budgets, sustainable management of water resources under a warming climate in the  
60 | harsh and the data-sparse Tibetan Plateau.

61

## 62 | **1 Introduction**

63 | As the highest plateau in the globe (the average elevation is higher than 4000 meters  
64 | above the sea level), the Tibetan Plateau (TP, also called “the roof of the world” or  
65 | “the third Pole”) is one of the most vulnerable region under a warming climate and is  
66 | subjected to strong interactions among atmosphere, hydrosphere, biosphere and  
67 | cryosphere in the earth system (Duan and Wu, 2006; Yao et al., 2012; Liu W. et al.,  
68 | 2016b). It also serves as the “Asian water tower” ~~with-from which~~ many major Asian  
69 | rivers such as Yellow ~~river~~River, Yangtze ~~river~~River, Brahmaputra ~~river~~River,  
70 | Mekong ~~river~~River, Indus ~~river~~River, etc., originate ~~from, which It~~ provides a vital  
71 | water resource to support hundreds of millions of people in China and the surrounding  
72 | countries (Immerzell et al., 2010; Zhang et al., 2013). Knowledge about the water  
73 | budgets and their responses to the changing environment is thus crucial for  
74 | understanding the hydrological regimes and for sustainable water resources  
75 | management as well as environmental protection in this special region (Yang et al.,  
76 | 2014; Chen et al., 2015).

77

78 | The TP is also known as a typical data-sparse mountain region which brings great  
79 | challenges to hydrological and related land surface studies (Zhang et al., 2007; Li F. et  
80 | al., 2013; Liu X. et al., 2016). For example, since the 1950s, totally 750 stations have  
81 | been established over China by the Chinese Meteorological Administration (CMA),  
82 | among which only less than 80 stations are distributed over the plateau (Wang and

83 Zeng, 2012). They are primary sparse and unevenly located at relatively low elevation  
84 regions, focus only on the meteorological variables and lack of other land surface  
85 observations such as evapotranspiration, snow water equivalent and latent heat fluxes,  
86 etc.. In addition, long-term consecutive observations of river discharge, snow depth,  
87 lake depth and glacier melts in the TP are also absent (Akhta et al., 2009; Ma et al.,  
88 2016). Therefore, the insights of water balance over various TP river basins ~~locates-~~  
89 located at different monsoon-dominant regions are, ~~to some extent,~~ still unclear so far  
90 ~~due to the lack of quantitative observations of the land surface processes~~ (Cuo et al.,  
91 2014; Xu et al., 2016). One way to ~~break-~~ overcome this limitation is to install more  
92 instruments to measure the ~~point scale~~ in situ water budgets (Yang et al., 2013; Zhou et  
93 al., 2013; Ma et al., 2015), but it is extremely expensive to maintain long-term  
94 observations at ~~the harsh environment and is often difficult to be applied to~~ basin or  
95 regional scales. Another ~~more popular way~~ workaround is to simulate basin-wide  
96 water budgets through physical-based land surface models at several large river basins  
97 forced with remote sensing data and large-scale gridded meteorological forcing  
98 datasets (Bookhagen and Burbank, 2010; Xue et al., 2013; Zhang et al., 2013; Cuo et  
99 al., 2015; Zhou et al., 2015; Wang et al., 2016). However, it is still difficult to use land  
100 surface models to multiple basins especially to the relatively smaller ones under  
101 complex terrains due to the lack of adequate data for model calibration and validation  
102 (Li F. et al., 2014).  
103 ~~it is also limited by the lack of adequate data for model calibration/validation and is~~  
104 ~~hard to be used to multiple basins especially to relatively smaller basins under the~~  
105 ~~complex terrains (Li F. et al., 2014).~~  
106  
107 ~~In recent years, a~~ number of global (or regional) datasets for water budget

108 | components have been released recently including remote sensing-based retrievals  
109 | (Tapley et al., 2004; Zhang et al., 2010; Long et al., 2014; Zhang Y. et al., 2016), land  
110 | surface model (LSM) simulations (Rui, 2011), reanalysis outputs (Berrisford et al.,  
111 | 2011; Kobayashi et al., 2015) and gridded forcing data interpolated from the in situ  
112 | observations (Harries et al., 2014). For example, there are considerable-many products  
113 | for terrestrial evapotranspiration (ET) such as GLEAM\_E (Global Land surface  
114 | Evaporation: the Amsterdam Methodology, Miralles et al., 2011a), MTE\_E (a product  
115 | integrated the point-wise ET observation at FLUXNET sites with geospatial  
116 | information extracted from surface meteorological observations and remote sensing in  
117 | a machine-learning algorithm, Jung et al., 2010 ), LSM-simulated ETs from Global  
118 | Land Data Assimilation System version 2 (GLDAS-2) with different land surface  
119 | schemes (Rodell et al., 2004), ETs from Japanese 55-year reanalysis (JRA55\_E), the  
120 | ERA-Interim global atmospheric reanalysis dataset (ERA-Interim) and the National  
121 | Aeronautic and Space Administration (NASA) Modern Era Retrospective-analysis  
122 | for Research and Application (MERRA) reanalysis data (Lucchesi, 2012). Moreover,  
123 | there are also several global or regional LSM-based runoff simulations from GLDAS  
124 | and the Variable Infiltration Capacity (VIC) model (Zhang et al., 2014). A few  
125 | attempts have been made to validate multiple datasets for certain water budget  
126 | components and to explore their possible hydrological implications, for example, Li X.  
127 | et al. (2014) and Liu W. et al. (2016a) evaluated multiple ET estimates against the  
128 | water balance method at annual and monthly time scales. Bai et al. (2016) assessed  
129 | streamflow simulations of GLDAS LSMs in five major rivers over the TP based on  
130 | the discharge observations. Although there are certain uncertainties among different  
131 | datasets with various spatial and temporal resolutions and calculated through different  
132 | algorithms (Xia et al., 2012), they do provide a great chance for us to quantify the

133 general basin-wide water budgets and their uncertainties in gauge-sparse regions such  
134 as the TP considered in this study.

135

136 The objectives of this study are (1) to investigate the general water budgets in 18 river  
137 basins across the Tibetan Plateau from the perspective of multiple datasets, and (2) to  
138 evaluate the seasonal cycles and annual trends of water budget components for 18 TP  
139 basins. The paper is organized as follows: the datasets and methods applied in this  
140 study are described in Sect.2. The results of season cycles and annual trends of water  
141 budget components for 18 TP basins are presented and discussed in Sect.3. The  
142 uncertainties inherited from multiple datasets are also discussed. In the Sect.4, we  
143 summarized the general results which would be helpful for understanding the water  
144 balances of the TP Rivers located at westerlies-dominated, Indian  
145 monsoon-dominated and East Asian monsoon-dominated regions.

146

## 147 **2 Data and Method**

### 148 **2.1 Multiple datasets used**

#### 149 **2.1.1 Study basins**

150 Eighteen river basins over the TP (Fig.1) with the drainage area ranging from 2832 to  
151 191235 km<sup>2</sup> (Table 1) are chosen in this study due to the availability of runoff data  
152 during the period 1982-2011. They mainly locate at the northwestern, southeastern  
153 and eastern parts of the plateau with multiyear-mean and basin-averaged temperature  
154 and precipitation ranging from -5.68 to 0.97 °C and 128 to 717 mm, which are solely  
155 or combined controlled by the westerlies, the Indian Summer monsoon and the Easter  
156 Asian monsoon (Yao et al., 2012). ~~The altitudes of the lowest and highest~~  
157 ~~hydrological gauging stations are 1650 m and 4982 m above the sea level.~~ The glacier

158 and snow covers are relatively more for the westerlies-dominant basins such as  
159 Yerqiang, Yulongkashi and Keliya (10.86~23.27% and 29.16~35.95%, respectively)  
160 whereas are less for the East Asian monsoon-dominated basins such as Yellow,  
161 Yangtze and Bayin (0~0.96% and 9.42~20.05%, respectively) (Table 1).

162 <Figure 1, here please, thanks>

163 <Table 1, here please, thanks>

### 164 2.1.2 Runoff, Precipitation and Terrestrial storage change

165 Observed daily runoff (Q) during the period 1982-2011 ~~used for water balance~~  
166 ~~calculation for 18 TP basins~~ was obtained from the National Hydrology Almanac of  
167 China (Table 2). There are < 30% missing data in some gauging stations such as  
168 Yajiang, Tongren, Gandatan and Zelingou. Therefore, the VIC Retrospective Land  
169 Surface Dataset over China (1952~2012, VIC\_IGSNRR simulated) with a spatial  
170 resolution of 0.25 degree and a daily temporal resolution from the Geographic  
171 Sciences and Natural Resources Research (IGSNRR), Chinese Academy of Sciences,  
172 is also used. ~~This dataset, which~~ is derived from the VIC model forced by the gridded  
173 daily observed forcing (IGSNRR\_forcing) (Zhang et al., 2014). A degree-day scheme  
174 was used in the model to consider the influences of snow and glacier on hydrological  
175 processes. ~~In this study, we first assess the VIC\_IGSNRR simulated runoff against the~~  
176 ~~observations for each basin (for example, at Tangnaihui and Pangduo stations in~~  
177 ~~Fig.2). The VIC\_IGSNRR simulated runoff is acceptable and could be used to replace~~  
178 ~~the missing values for a given basin, if the Nash Efficiency coefficient (NSE) between~~  
179 ~~the observation and simulation is above 0.65.~~

180 <Figure 2, here please, thanks>

181

182 Monthly gridded precipitation dataset (0.5 degree, 1961-2011) from CMA, which was



183 interpolated from observations of 2472 national meteorological stations using the  
184 Thin Plate Spline method, was used in this study (Table 2). Considering the  
185 uncertainty of CMA precipitation over the TP due to the relatively sparse stations ~~used~~  
186 and the complex terrain conditions, two other precipitation datasets (IGSNRR\_forcing  
187 and TRMM (Tropical Rainfall Measuring Mission) 3B43 V7, Huffman et al., 2012)  
188 were also ~~applied~~used. The precipitation from IGSNRR forcing datasets (0.25 degree)  
189 was derived by interpolating gauged daily precipitation from 756 CMA stations based  
190 on the synergraphic mapping system algorithm (Shepard, 1984; Zhang et al., 2014)  
191 and was further bias-corrected using the CMA gridded precipitation. ~~The CMA-~~  
192 ~~precipitation is perfectly consistent with TRMM (Corr = 0.86, RMSE = 8.34-~~  
193 ~~mm/month) and IGSNRR forcing (Corr = 0.94, RMSE = 7.15mm/month)-~~  
194 ~~precipitation for multiple basins (and also for the smallest basin above Tongren station,~~  
195 ~~Fig.2), which reveals the applicably of CMA precipitation under the TP conditions.-~~

196 <Table 2, here please, thanks>

197 Three latest global terrestrial water storage anomaly and water storage change ( $\Delta S$ )  
198 datasets (available on the GRACE Tellus website: <http://grace.jpl.nasa.gov/>) retrieved  
199 from the Gravity Recovery and Climate Experiment (GRACE, Tapley et al., 2004;  
200 Landerer and Swenson, 2012; Long et al., 2014), which were processed separately at  
201 the Jet Propulsion Laboratory (JPL), the GeoForschungsZentrum (GFZ) and the  
202 Center for Space Research at the University of Texas (CSR), were used. The GRACE  
203 retrievals (2002-2013) from three processing centers were averaged and a glacier  
204 isostatic adjustment correction as well a destriping filter were applied to minimize the  
205 errors and uncertainties of extracted  $\Delta S$ .

206

### 207 **2.1.3 Temperature, potential evaporation and ET**

208 The CMA monthly gridded temperature (0.5 degree) and potential evaporation (PET)  
209 dataset (0.5 degree, Harris et al., 2013) from Climatic Research Unit (CRU) in the  
210 University of East Anglia were used in this study. Moreover, six published  
211 global/regional ET products (four diagnostic products and two LSMs simulations,  
212 Table 2), namely (1) GLEAM\_E (Miralles et al., 2010, 2011), which estimated three  
213 sources of ET (transpiration, soil evaporation and interception) separately through  
214 bare soil, short vegetation and vegetation with a tall canopy through a set of algorithm  
215 ([www.gleam.eu](http://www.gleam.eu)), (2) GNoah\_E simulated by GLDAS-2 with the Catchment Noah  
216 scheme (<http://disc.sci.gsfc.nasa.gov/hydrology/data-holdings>) (Rodell et al., 2004),  
217 (3) Zhang\_E (Zhang et al., 2010) estimated using the modified Penman-Monteith  
218 approach forced with MODIS data, satellite-based vegetation parameters and  
219 meteorological observations (<http://www.ntsg.umd.edu/project/et>), (4) MET\_E (Jung  
220 et al., 2010) (<https://www.bgc-jena.mpg.de/geodb/projects/Home.phs>), (5) VIC\_E  
221 (Zhang et al., 2014) from VIC\_IGSNRR simulations  
222 ([http://hydro.igsnrr.ac.cn/public/vic\\_outputs.html](http://hydro.igsnrr.ac.cn/public/vic_outputs.html)) and (6) PML\_E (Zhang Y. et al.,  
223 2016) computed from global observation-driven Penman-Monteith-Leuning (PML)  
224 model (<https://data.csiro.au/dap/landingpage?pid=csiro:17375&v=2&d=true>).

225

#### 226 **2.1.4 Vegetation and snow/glacier parameters**

227 | ~~Two vegetation parameter datasets, t~~The Normalized Difference Vegetation Index  
228 (NDVI) and the Leaf Area Index (LAI) were used to quantify the dynamics of  
229 vegetation for 18 TP basins (Table 2). The NDVI data was obtained from the Global  
230 Inventory Modeling and Mapping Studies (GIMMS) (Turker et al., 2005)

231 ([https://nex.nasa.gov/nex/projects/1349/wiki/general\\_data\\_description\\_and\\_access/](https://nex.nasa.gov/nex/projects/1349/wiki/general_data_description_and_access/))  
232 while the LAI data was collected from the Global Land Surface Satellite (GLASS)  
233 products (<http://www.glcg.umd.edu/data/lai/>) (Liang and Xiao, 2012). Seasonal snow  
234 and glacier are widespread over the plateau which significantly influences the water  
235 and energy budgets in [the](#) TP, but their observations are difficult due to the harsh  
236 environment, especially at the basin scale. However, there are currently a few  
237 satellite-based or LSM-simulated products which could provide general information  
238 about the variations of snow and glacier. The daily cloud free snow composite product  
239 from MODIS Terra-Aqua and the Interactive Multisensor Snow and Ice Mapping  
240 System for the Tibetan Plateau was applied to quantify the snow cover changes for  
241 each basin (Zhang et al., 2012; Yu et al., 2015). The snow water equivalent (SWE)  
242 retrieved from Global Snow Monitoring for Climate Research product (GlobSnow-2,  
243 <http://www.globsnow.info/>) and the VIC\_IGSNRR simulations were also used in this  
244 study (Takala et al., 2011; Zhang et al., 2014). Moreover, the Second Glacier  
245 Inventory Dataset of China was used to extract the general distribution of glacier  
246 (Guo et al., 2014). All gridded datasets used were first uniformly interpolated to a  
247 spatial resolution of 0.5 degree [based on the bilinear interpolation](#) to make their  
248 inter-comparison possible. The datasets were then extracted for each of TP basins.

249

### 250 **2.1.5 Monsoon indices**

251 The TP climate is generally influenced by the westerlies, Indian summer monsoon and  
252 East Asian summer monsoon (Yao et al., 2012). To investigate the changes of  
253 monsoon systems and their potential influences on the water budget in [the](#) TP basins,  
254 three monsoon indices, namely Asian Zonal Circulation Index (AZCI), Indian Ocean  
255 Dipole Mode Index (IODMI) and East Asian Summer Monsoon Index (EASMI), are

256 | ~~also~~ used in this study. The IODMI is an indicator of the east-west temperature  
257 | gradient across the tropical Indian Ocean defined by Saji et al. (1999), which can be  
258 | downloaded from the following website:  
259 | [http://www.jamstec.go.jp/frcgc/research/d1/iod/HTML/Dipole%20Mode%20Index.ht](http://www.jamstec.go.jp/frcgc/research/d1/iod/HTML/Dipole%20Mode%20Index.html)  
260 | [ml](http://www.jamstec.go.jp/frcgc/research/d1/iod/HTML/Dipole%20Mode%20Index.html). The EASMI and AZCI (60°-150°E) reflect the dynamics of East Asian summer  
261 | monsoon (Li and Zeng, 2002) and the ~~westerlies~~westerly, which can be obtained from  
262 | the <http://ljp.gcess.cn/dct/page/65577> and the National Climate Center of China  
263 | (<http://ncc.cma.gov.cn/Website/index.php?ChannelID=43WCHID=5>), respectively.

## 264 | 2.2 Methods

### 265 | 2.2.1 Water balance-based ET estimation

266 | In this study, we first assess the VIC IGSNRR simulated runoff against the  
267 | observations for each basin (for example, at Tangnaihai and Pangduo stations in  
268 | Fig.2). The VIC IGSNRR simulated runoff is acceptable and could be used to replace  
269 | the missing values for a given basin, if the Nash Efficiency coefficient (NSE) between  
270 | the observation and simulation is above 0.65.

带格式的：居中

271 |  
272 | The basin-wide water balance at the monthly and annual timescales could  
273 | ~~traditionally~~ be written as the principle of mass conservation (also known as the  
274 | continuity equation, Oliverira et al., 2014) of basin-wide precipitation (P, mm),  
275 | evapotranspiration (ET<sub>wb</sub>, mm), runoff (Q, mm) as well as terrestrial water storage  
276 | change (ΔS, mm),

$$277 | \quad ET_{wb} = P - Q - \Delta S \quad (1)$$

278 | In most TP basins, glacier melt (M<sub>G</sub>, mm) contributes to river discharge together with  
279 | precipitation (liquid precipitation and snow). The monthly and annual water balance  
280 | in these basins can thus be revised as,

281 
$$ET_{wb} = P + M_G - Q - \Delta S \quad (2)$$

282 Several attempts have been made for separating glacier contributions to river  
283 discharge through site-scale isotopic observations, remote sensing as well as  
284 land-surface hydrological modeling for some individual TP basins (Zhang et al., 2013;  
285 Zhou et al., 2014; Neckel et al., 2014; [Xiang et al., 2016](#)). However, accurate  
286 quantification of  $M_G$  is difficult in [the](#) data-sparse TP, especially for multiple basins.  
287 In this study, we simply use the percentages of glacier melt to river discharge for  
288 some TP basins ~~concluded-derived~~ from the ~~existing-studies~~[literatures](#) (Chen, 1988;  
289 Mansur and Ajnis, 2005; Zhang et al., 2013; Liu J. et al., 2016) and the empirical  
290 relations between the glacier area ratio (%) and glacier melt in basins mentioned  
291 above (Table 3).

292 [<Table 3, here please, thanks>](#)

293 The terrestrial water storage ( $\Delta S$ ) in Eq.(2), which includes the surface, subsurface  
294 and ground water changes, cannot be neglected in water balance calculation at a  
295 monthly or annual timescale due to snow accumulation and some anthropogenic  
296 interferences such as reservoir regulation and agriculture irrigation (Liu W. et al.,  
297 2016a). The water balance-based ET ( $ET_{wb}$ ) during 2002-2011 can be calculated  
298 through Eq. (2) using the GRACE-derived mass anomaly as  $\Delta S$ . For  $ET_{wb}$   
299 calculation before 2002 when the GRACE data is unavailable, we use a two-step bias  
300 correction procedure (Li X. et al., 2014) to close the water balance ~~for 18 basins~~ at  
301 monthly timescale considering the  $\Delta S$ . We define  $P + M_G - Q$  as biased ET  
302 ( $ET_{biased}$ , available from 1982-2011) relative to the  $ET_{wb}$  (available from 2002-2011  
303 when the GRACE data is available) calculated from Eq. (2). Firstly, the  $ET_{biased}$  and  
304  $ET_{wb}$  series over the period 2002-2011 were separately fitted using a gamma  
305 distribution, which has been evidenced as an proper method for modeling the

306 probability distribution of ET (Bouraoui et al., 1999). The value in monthly  $ET_{biased}$   
307 series (2002-2011) can be bias-corrected through the inverse function ( $F^{-1}$ ) of the  
308 gamma cumulative distribution function (CDF,  $F$ ) of  $ET_{wb}$  by matching the  
309 cumulative probabilities between two CDFs as follow (Liu W. et al., 2016a),

$$310 \quad ET_{wb}(m) = F^{-1}(F(ET_{biased}(m)|\alpha_{biased}, \beta_{biased})|\alpha_{wb}, \beta_{wb}) \quad (3)$$

311 Here  $\alpha_{biased}$ ,  $\beta_{biased}$ ,  $\alpha_{wb}$  and  $\beta_{wb}$  are the shape and scale parameters of gamma  
312 distribution for  $ET_{biased}$  and  $ET_{wb}$ . The second step is to eliminate the annual bias  
313 through the ratio of annual  $ET_{biased}$  to annual  $ET_{wb}$  calculated in the first step using  
314 the following method,

$$315 \quad ET_{wb}(m) = \frac{ET_{biased(a)}}{ET_{wb(a)}} \times ET_{wb}(m) \quad (4)$$

316 The procedure was then applied to correct the monthly  $ET_{biased}$  series and calculated  
317 the monthly  $ET_{wb}$  during the period 1982-2001 for all TP basins. The  $ET_{wb}$  obtained  
318 was seemed as the “true” ET for evaluating multiple ET products and further for the  
319 trend analysis.

### 320 2.2.2 Modified Mann-Kendall test method

321 The Mann-Kendall (MK) test is a rank-based nonparametric approach ~~and which~~ is  
322 less sensitive to outlier relative to other parametric statistics. ~~However, it is, but~~  
323 ~~sometimes it is sometimes impacted-influenced~~ by the serial correlation of time series.  
324 Pre-whitening is often used to eliminate the influence of lag-1 autocorrelation before  
325 the use of MK test, for example, in pre-whitening, the analyzed time series  
326 ( $X_1, X_2, \dots, X_n$ ) will be replaced by ( $X_2 - cX_1, X_3 - cX_2, \dots, X_{n+1} - cX_n$ ) if the lag-1  
327 autocorrelation coefficient ( $c$ ) is larger than 0.1 (von Storch, 1995). However,  
328 significant lag-i autocorrelation may still be detected after pre-whitening because only  
329 the lag-1 autocorrelation is considered in pre-whitening (Zhang et al., 2013).  
330 Moreover, it sometimes underestimate the trend for a given time series (Yue et al.,

带格式的：字体：非倾斜

331 2002). Hamed and Rao (1998) proposed a modified version of MK test (MMK) to  
332 consider the lag- $j$  autocorrelation and related robustness of the autocorrelation through  
333 the use of equivalent sample size, which has been widely used in previous studies  
334 during the last five decades (McVicar et al., 2012; Zhang et al., 2013; Liu and Sun,  
335 2016).

带格式的: 字体: 非倾斜

336 In the MMK approach, if the lag- $j$  autocorrelation coefficients are significantly  
337 distinct from zero, the original variance of MK statistics will be replaced by the  
338 modified one. ~~In this study, we used a modified version of MK test (MMK, Hamed-~~  
339 ~~and Rao, 1998)the MMK approach~~ to quantify the trends of water budget components  
340 in 18 TP basins. ~~and the significance of trend was tested at the >95% confidence~~  
341 ~~level. The MMK considers the lag- $i$  autocorrelation and related robustness of the~~  
342 ~~autocorrelation, which has been widely used in previous studies during the last five~~  
343 ~~decades (McVicar et al., 2012; Liu and Sun, 2016).~~

带格式的: 字体: 非倾斜

### 345 **3 Results and Discussion**

#### 346 **3.1 ET evaluation and General hydrological characteristics of 18 TP basins**

347 In this study, we first assess the VIC\_IGSNRR simulated runoff against the  
348 observations for each basin (for example, at Tangnaihaid and Pangduo stations in  
349 Fig.2). The VIC\_IGSNRR simulated runoff is acceptable and could be used to replace  
350 the missing values for a given basin, if the Nash Efficiency coefficient (NSE) between  
351 the observation and simulation is above 0.65. Moreover, the CMA precipitation is  
352 consistent with TRMM (Corr = 0.86, RMSE = 8.34 mm/month) and IGSNRR forcing  
353 (Corr = 0.94, RMSE = 7.15mm/month) precipitation for multiple basins (and also for  
354 the smallest basin above Tongren station, Fig.2), which reveals the applicability of CMA  
355 precipitation under the TP conditions.

356 < Figure 2, here please, thanks >

357 We ~~first then~~ evaluated ~~monthly performances of~~ six ET products in 18 TP basins  
358 against ~~the our calculated~~  $ET_{wb}$  ~~at a monthly basis, which was calculated through~~  
359 ~~water balance considering the impacts of glacier and water storage change~~ (Fig. 3).

360 The ranges of monthly averaged ET among different basins (approximately 4–39 mm  
361 month<sup>-1</sup>) are very close for all products compare with that calculated from the  
362  $ET_{wb}$  (6–42 mm month<sup>-1</sup>). However, GLEAM\_E (correlation coefficient: Corr = 0.85  
363 and root-mean-square-error: RMSE = 5.69 mm month<sup>-1</sup>) and VIC\_E (Corr = 0.82 and  
364 RMSE = 6.16 mm month<sup>-1</sup>) perform relatively better than others. Although Zhang\_E  
365 and GNoah\_E were found closely correlated to monthly  $ET_{wb}$  in the upper Yellow  
366 River, the upper Yangtze River, Qiangtang and Qaidam basins (Li X. et al., 2014),  
367 they did not exhibit overall good performances (Corr = 0.61, RMSE = 7.97 mm  
368 month<sup>-1</sup> for Zhang\_E and Corr = 0.42, RMSE = 10.16 mm month<sup>-1</sup> for GNoah\_E) for  
369 18 TP basin used in this study. We thus use GLEAM\_E and VIC\_E together with  
370  $ET_{wb}$  to calculate the seasonal cycles and trends of ET in 18 TP basins in the  
371 following sections.

372 < Figure 3, here please, thanks >

373 To investigate the general hydro-climatic characteristics of rivers over the TP, we  
374 classify 18 basins into three categories, namely westerlies-dominated basins  
375 (Yerqiang, Yulongkashi and Kelia), Indian monsoon-dominated basins (Brahmaputra  
376 and Salween), and East Asian monsoon-dominated basins (Yellow, Yalong and  
377 Yangtze) referred to Tian et al. (2007) ~~and~~, Yao et al. (2012, ~~2013~~) and Dong et al.  
378 (2016). Interestingly, they are clustered into three groups under ~~the perspective of~~  
379 Budyko framework (Budyko, 1974; Zhang D. et al., 2016) with relatively lower  
380 evaporative index for Indian monsoon-dominant basins and higher aridity index for



381 | westerlies-dominant basins, which reveal various long-term hydro-climatologic  
382 | conditions (Fig. 4). Overall, the annual mean air temperature increases (-5.68 ~0.97 °C)  
383 | while multiyear mean glacier area (and thus the glacier melt normalized by  
384 | precipitation) decreases (23.27 ~ 0%) gradually from the westerlies-dominant, Indian  
385 | monsoon-dominant to East Asian monsoon-dominant basins. The vegetation status  
386 | (NDVI range: 0.05~0.43; LAI range: 0.03~0.83) tends to be better and ET increases  
387 | (and thus runoff coefficient gradually decreases) from cold to warm basins (Fig. 4 and  
388 | Table 1). The  $R^2$  between basin-averaged NDVI and ET is 0.76 which shows a clear  
389 | vegetation control on ET in 18 TP basins. The result is in line with Shen et al. (2015),  
390 | which indicated that the spatial pattern of ET trend was significantly and positively  
391 | correlated with NDVI trend over the TP. It is a general picture of hydrological regime  
392 | in high-altitude and cold regions (Zhang et al., 2013; Cuo et al., 2014), which could  
393 | be interpreted from the perspective of multi-source datasets in the data-sparse TP.

带格式的：上标

394 | < Figure 4, here please, thanks >

### 395 | 3.2 Seasonal cycles of basin-wide water budget components for the TP basins

396 | The multi-year means of water budget components (i.e., P, Q, ET, snow cover and  
397 | SWE) and vegetation parameters (i.e., NDVI and LAI) were calculated for each  
398 | calendar month and for 18 TP river basins ~~over~~ using multi-source datasets available  
399 | from 1982 to 2011. Overall, the seasonal variations of P, Q, ET, air temperature and  
400 | vegetation parameters are similar in all TP basins with peak values occurred in May to  
401 | September (Fig.5 and Fig.6). The seasonal cycles of snow cover and SWE are  
402 | generally time consistent as well for 18 TP basins (the peak values mainly occur from  
403 | October to next April, Fig.7). With the ascending air temperature from cold to warm  
404 | months, the basin-wide precipitation increases and vegetation turns green gradually  
405 | (the basin-wide ET also increase). Meanwhile, glacier and snow melt or vanish

406 gradually with the melt water supply the river discharge together with precipitation.  
407 The inter-basin variations of hydrological regime are to a large extent linked to the  
408 climate systems that prevail over the TP.

409 [< Figure 5, here please, thanks >](#)

410 Although the temporal patterns of hydrological components are general analogous,  
411 they varied among parameters, climate zones and even basins (Zhou et al., 2005). For  
412 example, relative to air temperature, the seasonal variation of runoff is more similar to  
413 precipitation which reveals that runoff is mainly controlled by precipitation in ~~the~~  
414 most TP basins. It is in agreement with that summarized by Cuo et al. (2014). In the  
415 westerlies-dominated basins, the peak values of precipitation and runoff mainly  
416 concentrate in June-August, which contribute approximately 68-82% and 67-78% of  
417 annual totals, respectively. During this period, the runoff always exceeds precipitation  
418 which indicates large contributions of glacier/snow-melt water to streamflow. It is  
419 consistent with the existing findings in Tarim River (Yerqiang, Yulongkashi and  
420 Keliya rivers are the major tributaries of Tarim River), which indicated that the melt  
421 water accounted for about half of the annual total streamflow (Fu et al., 2008). The  
422 ET (vegetation cover) in three westerlies-dominated basins are relatively less (scarcer)  
423 than that in other TP basins while the percentages of glacier and seasonal snow cover  
424 are higher in these basins which contribute more melt water to river discharge (Fig.6  
425 and Fig.7). Overall, the SWE in Yerqiang, Yulongkashi and Keliya rivers are  
426 relatively higher in winter than other seasons, but they vary with basins and products  
427 which reveal considerable uncertainties in SWE estimations.

428 [< Figure 6, here please, thanks >](#)

429 In the Indian monsoon and East Asian monsoon-dominated basins, the runoff  
430 concentrates during June-September (~~-or June- June-October~~) with precipitation being

431 the dominant contributor of annual total runoff. For example, the peak values of  
432 precipitation and runoff occur during June-September at Zhimenda station  
433 (contributing about 80% and 74% of the annual totals) while those occur during  
434 June-October at Tangnaihai station (contributing about 78% and 71% of the annual  
435 totals, respectively). The results are quite similar to the related studies in eastern and  
436 southern TP such as Liu (1999), Dong et al. (2007), Zhu et al. (2011), Zhang et al.  
437 (2013), Cuo et al. (2014). The vegetation cover (ET) in most basins is relatively better  
438 (higher) than that in the westerlies-dominant basins. Moreover, the seasonal snow  
439 mainly covers from mid-autumn to spring and correspondingly the SWE is relatively  
440 higher in these months in all basins except for Yellow River above Xining station,  
441 Salwee River above Jiayuqiao station and Brahmaputra River above Nuxia and  
442 Yangcun stations.

443 < Figure 7, here please, thanks >

### 444 3.3 Trends of basin-wide water budget components for the TP basins

445 Trends in water budget components for 18 TP basins during the period 1982-2011  
446 were also examined through the modified Mann-Kendall test (MMK) in this study.  
447 The hydrological cycles intensified in the westerlies-dominated basins with Q, P and  
448  $ET_{wb}$  all ascended with regional warming (Fig.8), especially in the Keliya River  
449 basin (Numaitilangan station). The aridity index (PET/P), which is an indicator for the  
450 degree of dryness, slightly declined in all basins in northwestern TP. Although P and  
451 PET were found both increase since the 1980s~~The results were in line with the overall~~  
452 ~~climate warming and moistening reported in northwest China~~ (Shi et al., 2003; Yao et  
453 al., 2014), ~~at which these basins located.~~ the declined PET/P is, to some extent,  
454 attributed to the ascending P exceed the increase in PET for these basins (except for  
455 the Yulongkashi basin). The climate moistening in the headwaters of these inland

456 | rivers would be beneficial to the water resources and oasis agro-ecosystems in the  
457 | middle and lower basins. –The increase in streamflow was also found in most  
458 | tributaries of the Tarim River (Sun et al., 2006; Fu et al., 2010; Mamat et al., 2010).  
459 | Moreover, the westerlies, revealed by the Asian Zonal Circulation Index (60°-150° E),  
460 | slightly enhanced (linear trend: 0.21) over the period of 1982-2011 (Fig.9). More  
461 | water vapor was transported and fell as precipitation or snow in northwestern TP (e.g.,  
462 | the eastern Pamir region) with the strengthening westerlies. Both SWE products  
463 | (VIC\_IGSNRR simulated and GlobaSnow-2 product) showed slightly increase for all  
464 | basins~~The SWE showed increase for all basins and for both products (VIC\_IGSNRR-~~  
465 | ~~simulated and GlobaSnow-2 product)~~ with the incremental seasonal snow cover and  
466 | advanced glaciers (Yao et al., 2012). More precipitation was transformed into snow or  
467 | glacier and the runoff coefficient (Q/P) exhibited decrease although precipitation  
468 | obviously increased (Fig.8). In addition, the transpiration in these basins may decrease  
469 | with vegetation degradation revealed by the NDVI and LAI (Yin et al., 2016) but the  
470 | atmospheric evaporative demand indicated by CRU PET increased (significantly  
471 | increase in the Yulongkashi and Keliya rivers) during the period 1982-2011.

472 | < [Figure 8, here please, thanks](#)>

473 | < [Figure 9, here please, thanks](#)>

474 | In the East Asian monsoon-dominated basins, there are two types of change for  
475 | basin-wide water budget components. For example, P and Q slightly decreased in the  
476 | upper Yellow River (Tangnihai, Huangheyan and Jimai stations) and Yalong River  
477 | (Yajiang station) but increased in other basins (Zelingou, Gandatan, Xining, Tongren  
478 | and Zhimenda stations) over the period of 1982-2011 (Fig.10). The decline in Q and P  
479 | for the upper Yellow and Yalong Rivers (locate at the eastern Tibetan Plateau) were  
480 | consistent with that found by Cuo et al. (2013, 2014) as well as Yang et al. (2014), and

481 were in line with the weakening (linear slope: -0.01) of the East Asian Summer  
482 Monsoon (Fig.9). The vegetation turned green while  $ET_{wb}$  and PET increased in all  
483 nine basins with the significantly ascending air temperature during the period  
484 1982-2011. The aridity index (PET/P) was found decrease in all basins except for the  
485 upper Yellow River basin above Jimai station and the upper Yalong River basin above  
486 Yajiang station. Moreover, ~~the both the~~ runoff coefficients and SWE (SWE) were  
487 decrease ~~(decrease~~ except for the Bayin River above Zelingou station and the upper  
488 Yellow River above Tongren station) in the East Asian monsoon dominated basins.

489 < Figure 10, here please, thanks >

490 The hydrological cycles were also found intensified in the Indian monsoon-dominated  
491 basins such as Salween River and Brahmaputra River (Fig.11), which were in line  
492 with the strengthen (linear trend: 0.000601) of the Indian Summer monsoon (revealed  
493 by the Indian Ocean Dipole Mode Index) during the specific period 1982-2011 (Fig.9).  
494 In the six basins, trends in P, Q and  $ET_{wb}$  were all upward. For example, at  
495 Jiayuqiao station, the annual streamflow showed slightly increasing trend which was  
496 consistent with that examined during 1980-2000 by Yao et al. (2012). The vegetation  
497 status, revealed by NDVI and LAI, turned better significantly with the ascending air  
498 temperature. The aridity index (PET/P) decreased in all basins except for the  
499 Brahmaputra River above Tangjia station, which indicated that most basins in the  
500 Indian monsoon-dominated regions turn wet over the period of 1982-2011. The runoff  
501 coefficient (Q/P) increased at Gongbujiangda and Nuxia while decreased at Jiayuqiao,  
502 Pangduo, Tangji and Yangcun stations. Moreover, the basin-wide SWE declined in the  
503 upper Salween River and Brahmaputra River above Pangduo, Tangjia and  
504 Gongbujiangda stations while increased in Brahmaputra River above Nuxia and  
505 Yangcun stations.

506

< Figure 11, here please, thanks >

### 507 3.4 Uncertainties

508 The results may unavoidably associate with several aspects of ~~uncertainties-~~  
509 uncertainty which mainly inherited from the multi-source datasets used. ~~For example,-~~  
510 ~~a~~Although both GLEAM\_E and VIC\_E captured the ~~the~~ seasonal cycles of  $ET_{wb}$  ~~can-~~  
511 ~~be captured by GLEAM\_E and VIC\_E,~~ they still have considerable uncertainties ~~such-~~  
512 ~~as~~ at such as Numaitilangan, Gongbujiangda and Nuxia stations (Fig.5). With respect  
513 to the annual trend of  $ET_{wb}$  (Table 4), most ET products (including the  
514 well-performed GLEAM\_E and VIC\_E in some basins) cannot detect the decreasing  
515 trends in 7 out of 18 basins (e.g., at Kulukelangan, Tongguziluoke, Xining, Tongren,  
516 Jimai, Nuxia and Gongbujiangda stations) due to their uncertainties inherited from  
517 different forcing data, algorithm used and varied spatial-temporal resolutions (Li et al.,  
518 2014; Liu W et al., 2016a). ~~-~~In particular, it is well known that land surface models  
519 have some difficulties (e.g., parameter tuning in boundary layer schemes) when  
520 applying to the TP (Xia et al., 2012; Bai et al., 2016). For example, Xue et al. (2013)  
521 indicated that GNoah\_E underestimated the  $ET_{wb}$  in the upper Yellow River and  
522 Yangtze River basins on the Tibetan Plateau mainly due to its negative-biased  
523 precipitation forcing. We thus only used  $ET_{wb}$  in the trend detection of water budget  
524 components in Fig.8, Fig.10 and Fig.11 in this study.  
525 ~~The two SWE products also showed large uncertainty, with respect to both their~~  
526 ~~seasonal cycles and trends due to their different forcing data; different algorithms-~~  
527 ~~applied as well as varied spatial temporal resolutions.-~~The VIC\_IGSNRR simulated  
528 and GlobaSnow-2 snow water equivalents have also not been validated in the TP due  
529 to the lack of in situ observations. However, they showed similar seasonal cycles and  
530 annual trends in some basins such as Zelingou and Numaitilangan, which revealed

531 | the applicability of the SWE products for these basins. Moreover, the interpolation of  
532 | missing values of runoff with VIC\_IGSNRR simulated runoff and the gridded  
533 | precipitation data (which interpolated from limited gauged precipitation over the  
534 | plateau) involved some uncertainties as well as. Finally, we obtained the contributions  
535 | of glacier-melt to discharge in some basins from the literatures and took them as fixed  
536 | numbers. It may inherit considerable uncertainty from varied studies using different  
537 | approaches such as glacier mass-balance observation, isotope observation and  
538 | hydrological modeling, and the contribution rates would also change under a warming  
539 | climate. However, accurate quantification of the contribution of glacier-melt to  
540 | discharge is technically difficult nowadays, especially for the data-sparse basins.  
541 | ~~However, w~~With these caveats, we can interpret the general hydrological regimes and  
542 | their responses to the changing climate in the TP basins from solely the perspective of  
543 | multi-source datasets, which are comparable to the existing studies based on the in  
544 | situ observations and complex hydrological modeling.

545 | <Table 4, here please, thanks>

#### 546 | **4 Summary**

547 | In this study, we investigated the seasonal cycles and trends of water budget  
548 | components in 18 TP basins during the period 1982-2011, which is not well  
549 | understood so far due to the lack of adequate observations in the harsh environment,  
550 | through integrating the multi-source global/regional datasets such as gauge data,  
551 | satellite remote sensing and land surface model simulations. By using a two-step bias  
552 | correction procedure, annual basin-wide  $ET_{wb}$  was calculated through the water  
553 | balance considering the impacts of glacier and water storage change. The GLEAM\_E  
554 | and VIC\_E were found perform better relative to other products against the  
555 | calculated  $ET_{wb}$ .

556

557 The general water and energy budgets were different in the westerlies-dominated  
558 (with higher aridity index, runoff coefficient and glacier cover), the Indian  
559 monsoon-dominated and the East Asian monsoon-dominated (with higher air  
560 temperature, vegetation cover and evapotranspiration) basins under the perspective of  
561 Budyko framework. In 18 TP basins, precipitation is the major contributor to the river  
562 runoff, which concentrates mainly during June-October (June-August for the  
563 westerlies-dominated basins, June-September or June to October for the Indian  
564 monsoon-dominated and the East Asian monsoon-dominated basins). The basin-wide  
565 SWE is relatively higher from mid-autumn to spring for all 18 TP basins except for  
566 Keliya River and Brahmaputra River above the Nuxia and Yangcun stations. The  
567 vegetation cover is relatively less whereas snow/glacier cover is more in the  
568 westerlies-dominant basins compared with other basins. The hydrological cycles were  
569 found intensified under the regional warming in most TP basins except for most  
570 tributaries of the upper Yellow River and the Yalong River, which were significantly  
571 influenced by the weakening East Asian monsoon during the period 1982-2011. The  
572 aridity index (PET/P) exhibited decrease in most TP basins which corresponded to the  
573 warming and moistening climate in the TP and western China. Moreover, the runoff  
574 coefficient (Q/P) declined in most basins which may be, to some extent, due to ET  
575 increase induced by vegetation greening and the influences of snow and glacier  
576 changes. Although there are considerable uncertainties inherited from multi-source  
577 data used, the general hydrological regimes in [the](#) TP basins could be revealed, which  
578 are consistent to the existing results obtained from in situ observations and complex  
579 land surface modeling. It indicated the usefulness of integrating the multiple datasets  
580 available such as in situ observations, remote sensing-based products, reanalysis



581 outputs, land surface model simulations and climate model outputs for hydrological  
582 applications. The results obtained could be helpful for understanding the hydrological  
583 eyeles,cycles and further for the water resources management and eco-environment  
584 protection under a warming climate in the vulnerable Tibetan Plateau.

585

586 ***Author contributions.*** Wenbin Liu and Fubao Sun developed the idea to see the  
587 general water budgets in the TP basins from the perspective of multisource datasets.  
588 Wenbin Liu collected and processed the multiple datasets with the help of Yanzhong  
589 Li, Guoqing Zhang, Hong Wang as well as Peng Bai, and prepared the manuscript.  
590 The results were extensively commented and discussed by Fubao Sun, Jiahong Liu  
591 and Yan-Fang Sang.

592

593 ***Acknowledgements.*** This study was supported by the National Key Research and  
594 Development Program of China (2016YFC0401401 and 2016YFA0602402), National  
595 Natural Science Foundation of China (41401037 and 41330529), the Open Research  
596 Fund of State Key Laboratory of Desert and Oasis Ecology in Xinjiang Institute of  
597 Ecology and Geography, Chinese Academy of Sciences (CAS), the CAS Pioneer  
598 Hundred Talents Program (Fubao Sun), the Initial Founding of Scientific Research  
599 (Y5V50019YE) and the program for the “Bingwei” Excellent Talents from the  
600 Institute of Geographic Sciences and Natural Resources Research, CAS. We are  
601 grateful to the NASA MEaSUREs Program (Sean Swenson) for providing the  
602 GRACE land data processing algorithm. The basin-wide water budget series in the TP  
603 Rivers used in this study are available from the authors upon request  
604 ([liuwb@igsnr.ac.cn](mailto:liuwb@igsnr.ac.cn)). We wish to thank the editors and reviewers for their invaluable  
605 comments and constructive suggestions to improve the quality of the manuscript.

606

607 **References**

- 608 Akhtar, M., Ahmad, N., and Booij, M.J.: Use of regional climate model simulations as input for  
609 hydrological models for the Hindukush-Karakorum-Himalaya region, *Hydrol. Earth Syst. Sci.*  
610 13, 1075-1089, 2009.
- 611 Bai, P., Liu, X.M., Yang, T.T., Liang, K., and Liu, C.M.: Evaluation of streamflow simulation  
612 results of land surface models in GLDAS on the Tibetan Plateau, *J. Geophys. Res. Atmos.*, 121,  
613 12180-12197, 2016.
- 614 Berrisford, P, Lee, D., Poli, P., Brugge, R., Fielding, K., Fuentes, M., Kallberg, P., Kobayashi, S.,  
615 Uppala, S., and Simmons, A.: The ERA-interim archive. ERA Reports Series No. 1 Version 2.0,  
616 Available from: [https://www.researchgate.net/publication/41571692\\_The\\_ERA-interim](https://www.researchgate.net/publication/41571692_The_ERA-interim_archive)  
617 archive>, 2011.
- 618 Bookhagen, B. and Burbank, D.W.: Toward a complete Himalayan hydrological budget:  
619 spatiotemporal distribution of snowmelt and rainfall and their impact on river discharge, *J.*  
620 *Geophys. Res.*, 115, F03019, 2010.
- 621 Bouraoui, F., Vachaud, G., Li, L.Z.X., LeTreut, H., and Chen, T.: Evaluation of the impact of  
622 climate changes on water storage and groundwater recharge at the watershed scale, *Clim. Dyn.*,  
623 15(2), 153-161, 1999.
- 624 Budyko, M.I.: *Climate and life*. Academic Press, 1974.
- 625 Chen, D., Xu, B., Yao, T., Guo, Z., Cui, P., Chen, F., Zhang, R., Zhang, X., Zhang, Y., Fan, J., Hou,  
626 Z., and Zhang, T.: Assessment of past, present and future environmental changes on the Tibetan  
627 Plateau, *Chinese SCI. Bull.*, 60(32), 3025-3035, 2015 (in Chinese).
- 628 Chen, J.: Lichenometrical studies on glacier changes during the Holocene Epoch at the sources  
629 region of Urumqi River, *Sci. China B.*, 18(1), 95-104, 1988 (in Chinese).
- 630 Cuo, L., Zhang, Y.X., Bohn, T.J., Zhao, L., Li, J.L., Liu, Q.M., and Zhou, B.R.: Frozen soil  
631 degradation and its effects on surface hydrology in the northern Tibetan Plateau, *J. Geophys.*  
632 *Res. Atmos.*, 120(6), 8276-8298, 2015.
- 633 Cuo, L., Zhang, Y.X., Gao, Y., Hao, Z., and Cairang, L.: The impacts of climate change and land  
634 cover/use transition on the hydrology in the upper Yellow River Basin, China, *J. Hydrol.*, 502,  
635 37-52, 2013.

636 Cuo, L., Zhang, Y.X., Zhu, F.X., and Liang, L.Q.: Characteristics and changes of streamflow on  
637 the Tibetan Plateau: A review, *J. Hydrol. Reg. stud.*, 2, 49-68, 2014.

638 Dong, X., Yao, Z., and Chen, C.: Runoff variation and responses to precipitation in the source  
639 regions of the Yellow River, *Resour. Sci.*, 29(3), 67-73, 2007 (in Chinese).

640 [Dong, W., Lin, Y., Wright, J.S., Ming, Y., Xie, Y., Wang, B., Luo, Y., Huang, W., Huang, J., Wang,](#)  
641 [L., Tian, L., Peng, Y., and Xu, F.: Summer rainfall over the southwestern Tibetan Plateau](#)  
642 [controlled by deep convection over the Indian Subcontinent, \*Nat. Commun.\*, 7, 10925, 2016.](#)

643 Duan, A.M. and Wu, G.X.: Change of cloud amount and the climate warming on the Tibetan  
644 Plateau, *Geophys. Res. Lett.*, 33, L22704, 2006.

645 Fu, L., Chen, Y., Li, W., Xu, C., and He, B.: Influence of climate change on runoff and water  
646 resources in the headwaters of the Tarim River, *Arid Land Geogr.*, 31(2), 237-242, 2008 (in  
647 Chinese).

648 Fu, L., Chen, Y., Li, W., He, B., and Xu, C.: Relation between climate change and runoff volume  
649 in the headwaters of the Tarim River during the last 50 years., *J. Desert Res.*, 30(1), 204-209,  
650 2010 (in Chinese).

651 Guo, W.Q., Liu, S.Y., Yao, X.J., Xu, J.L., Shangguan, D.H., Wu, L.Z., Zhao, J.D., Liu, Q., Jiang,  
652 Z.L., Wei, J.F., Bao, E.J., Yu, P.C., Ding, L.F., Li, G., Ge, C.M., and Wang, Y.: The Second  
653 Glacier Inventory Dataset of China, Cold and Arid Regions Science Data Center at Lanzhou,  
654 doi: 10.3972/glacier.001.2013.db, 2014.

655 Hamed, K.H. and Rao, A.R.: A modified Mann-Kendall trend test for autocorrelation data,  
656 *J.Hydrol.*, 204(1-4), 182-196, 1998.

657 Huffman, G.J., , E.F., Bolvin, D.T., Nelkin, E.J., and Adler, R.F.: last updated 2013: TRMM  
658 Version 7 3B42 and 3B43 Data Sets, NASA/GSFC, Greenbelt, MD. Data set accessed at  
659 <http://mirador.gsfc.nasa.gov/cgi-bin/mirador/>  
660 [presentNavigation.pl?tree=project&project=TRMM&dataGroup=Gridded&CGIS](http://mirador.gsfc.nasa.gov/cgi-bin/mirador/presentNavigation.pl?tree=project&project=TRMM&dataGroup=Gridded&CGIS)  
661 [ESSID=5d12e2ffa38ca2aac6262202a79d882a](http://mirador.gsfc.nasa.gov/cgi-bin/mirador/presentNavigation.pl?tree=project&project=TRMM&dataGroup=Gridded&CGIS), 2012.

662 Harris, I., Jones, P.D., Osborn, T.J., and Lister, D.H.: Updated high-resolution grids of monthly  
663 climatic observations – the CRU TS3.10 Dataset, *Int. J. Climatol.*, 34 (3), 623-642, 2014.

664 Immerzeel, W.W., van Beek, L.P.H., and Bierkens, M.F.P.: Climate change will affect the Asian  
665 water towers, *Science*, 328, 1382-1385, 2010.

666 Jung, M., Reichstein, M., Ciais, P., Seneviratne, S.I., Sheffield, J., Goulden, M.L., Bonan, G.,  
667 Cescatti, A., Chen, J., de Jeu, R., Dolman, A.J., Eugster, W., Gerten, D., Gianelle, D., Gobron, N.,  
668 Heinke, J., Kimball, J., Law, B.E., Montagnani, L., Mu, Q., Mueller, B., Oleson, K., Papale, D.,  
669 Richardson, A.D., Rouspard, O., Running, S., Tomelleri, E., Viovy, N., Weber, U., Williams, C.,  
670 Wood, E., Zaehle, S., and Zhang, K.: Recent decline in the global land evapotranspiration trend  
671 due to limited moisture supply, *Nature*, 467, 951-954, 2010.

672 Kobayashi, S., Ota, Y., Harada, Y., Ebita, A., Moriya, M., Onoda, H., Onogi, K., kamahori, H.,  
673 kobayashi, C., Endo, H., miyaoka, K., and Takahashi, K.: The JRA-55 Reanalysis: General  
674 specifications and basic characteristics, *J.Meteor. Soc. Japan*, 93(1), 5-58, doi:  
675 10.2151/jmsj.2015-001, 2015.

676 Landerer, F.W. and Swenson, S.C.: Accuracy of scaled GRACE terrestrial water storage estimates,  
677 *Water Resour.Res.*, 48, W04531, 2012.

678 Li, F.P., Zhang, Y.Q., Xu, Z.X., Liu, C.M., Zhou, Y.C., and Liu, W.F.: Runoff predictions in  
679 ungauged catchments in southeast Tibetan Plateau, *J. Hydrol.*, 511, 28-38, 2014.

680 Li, F.P., Zhang, Y.Q., Xu, Z.X., Teng, J., Liu, C.M., Liu, W.F., and Mpelasoka, F.: The impact of  
681 climate change on runoff in the southeastern Tibetan Plateau, *J. Hydrol.*, 505, 188-201, 2013.

682 Li, J.P. and Zeng, Q.C.: A unified monsoon index, *Geophys. Res. Lett.*, 29(8), 1274, 2002.

683 Li, X.P., Wang, L., Chen, D.L., Yang, K., and Wang, A.H.: Seasonal evapotranspiration changes  
684 (1983-2006) of four large basins on the Tibetan Plateau, *J. Geophys. Res.*, 119 (23),  
685 13079-13095, 2014.

686 Liang, S.L. and Xiao, Z.Q.: Global Land Surface Products: Leaf Area Index Product Data  
687 Collection(1985-2010), Beijing Normal University, doi:10.6050/glass863.3004.db, 2012.

688 Liu, J., Liu, T., Bao, A., De Maeyer, P., Feng, X., Miller, S.N., and Chen, X.: Assessment of  
689 different modeling studies on the spatial hydrological processes in an arid alpine catchment,  
690 *Water Resour. Manag.*, 30, 1757-1770, 2016.

691 Liu, T.: Hydrological characteristics of Yalungzangbo River, *Acta Geogr. Sin.*, 54 (Suppl.),  
28 / 56

692 157-164, 1999 (in Chinese).

693 Liu, W.B. and Sun, F.B.: Assessing estimates of evaporative demand in climate models using  
694 observed pan evaporation over China, *J. Geophys. Res. Atmos.*, 121, 8329-8349, 2016.

695 Liu, W.B., Wang, L., Zhou, J., Li, Y.Z., Sun, F.B., Fu, G.B., Li, X.P., and Sang, Y-F.: A worldwide  
696 evaluation of basin-scale evapotranspiration estimates against the water balance method, *J.*  
697 *Hydrol.*, 538, 82-95, 2016a.

698 Liu, W.B., Wang, L., Chen, D.L., Tu, K., Ruan, C.Q., and Hu, Z.Y.: Large-scale circulation  
699 classification and its links to observed precipitation in the eastern and central Tibetan Plateau,  
700 *Clim. Dyn.*, 46, 3481-3497, 2016b.

701 Liu, X.M., Yang, T., Hsu, K., Liu, C., and Sorooshian, S.: Evaluating the streamflow simulation  
702 capability of PERSIANN-CDR daily rainfall products in two river basins on the Tibetan Plateau,  
703 *Hydrol. Earth Syst. Sci. Discuss.*, doi: 10.5194/hess-20160282, 2016.

704 Long, D., shen, Y.J., Sun, A., Hong, Y., Longuevergne, L., Yang, Y.T., Li, B., and Chen, L.:  
705 Drought and flood monitoring for a large karst plateau in Southwest China using extended  
706 GRACE data, *Remote Sen. Environ.*, 155, 145-160, 2014.

707 Lucchesi, R.: File specification for MERRA products, GMAO Office Note No.1 (version 2.3), 82  
708 pp, available from [http://gmao.gsfc.nasa.gov/pubs/office\\_notes](http://gmao.gsfc.nasa.gov/pubs/office_notes), 2012.

709 Ma, N., Szilagyi, J., Niu, G.Y., Zhang, Y.S., Zhang, T., Wang, B.B., and Wu, Y.H.: Evaporation  
710 variability of Nam Co Lake in the Tibetan Plateau and its role in recent rapid lake expansion, *J.*  
711 *Hydrol.*, 537, 27-35, 2016.

712 Ma, N., Zhang, Y.S., Guo, Y.H., Gao, H.F., Zhang, H.B., and Wang, Y.F.: Environmental and  
713 biophysical controls on the evapotranspiration over the highest alpine steppe, *J. Hydrol.*, 529,  
714 980-992, 2015.

715 Mamat, A., Halik, W., and Yang, X.: The climatic changes of Qarqan river basin and its impact on  
716 the runoff, *Xinjiang Agric. Sci.*, 47 (5), 996-1001, 2010 (in Chinese).

717 Mansur, S. and Ajinisa, T.: An analysis of water resources and it's hydrological characteristics of  
718 Yarkend River Valley, *J. Xinjiang Norm. Univ. (Nat. Sci. Ed.)*, 24(1), 74-78, 2005 (in Chinese).

719 McVicar, T.R., Roderick, M., Donohue, R.J., Li, L.T., Van Niel, T.G., Thomas, A., Grieser, J.,  
720 Jhajharia, D., Himri, Y., Mahowald, N.M., Mescherskaya, A.V., Kruger, A.C., Rehman, S., and  
29 / 56

721 Dinpashoh, Y.: Global review and synthesis of trends in observed terrestrial near-surface wind  
722 speeds: implications for evaporation, *J. Hydrol.*, 416-417, 182-205, 2012.

723 Miralles, D.G., De Jeu, R.A.M., Gash, J.H., Holmes, T.R.H., and Dolman, A.J.: Magnitude and  
724 variability of land evaporation and its components at the global scale, *Hydrol. Earth Syst. Sci.*, 15,  
725 967-981, 2011.

726 Miralles, D.G., Gash, J.H., Holmes, T.R.H., de Jeu, R.A.M, and Dolman, A.J.: Global canopy  
727 interception from satellite observations, *J. Geophys. Res.*, 115, D16122, 2010.

728 Neckel, N., Kropáčková, J., Bolch, T., and Hochschild, V.: Glacier mass changes on the Tibetan  
729 Plateau 2003-2009 derived from ICESat laser altimetry measurements, *Environ. Res. Lett.*, 9,  
730 014009(7pp), 2014.

731 Oliveira, P.T.S., Mearing, M.A., Moran, M.S., Goodrich, D.C., Wendland, E., and Gupta, H.V.:  
732 Trends in water balance components across the Brazilian Cerrado, *Water Resour. Res.*, 50,  
733 7100-7114, 2014.

734 Rodell, M., Houser, P.R., Jambor, U., Gottschalck, J., Mitchell, K., Meng, C.-J., Arsenault, K.,  
735 Cosgrove, B., Radakovich, J., Bosilovich, M., Entin, J.K., Walker, P., Lohmann, D., and Toll, D.:  
736 The global land data assimilation system, *B. Am. Meteorol. Soc.*, 85, 381-394, 2004.

737 Rui, H.: README Document for Global Land Data Assimilation System Version 2 (GLDAS-2)  
738 Products, GES DISC, 2011.

739 Saji, N.H., Goswami, B.N., Vinayachandran, P.N., and Yamagata, T.: A dipole mode in the tropical  
740 Indian Ocean, *Nature*, 401, 360-363, 1999.

741 [Shen, M.G., Piao, S.L., Jeong, S., Zhou, L.M., Zeng, Z.Z., Ciais, P., Chen, D.L., Huang, M.T., Jin,](#)  
742 [C.S., Li, L.Z.X., Li, Y., Myneni, R.B., Yang, K., Zhang, G.X., Zhang, Y.J., and Yao, T.D.:](#)  
743 [Evaporative cooling over the Tibetan Plateau induced by vegetation growth, \*Proc. Natl. Acad.\*](#)  
744 [Sci. U. S.A., 112\(30\), 9299-9304, 2015.](#)

745 Shi, Y.F., Shen, Y.P., Li, D.L., Zhang, G.W., Ding, Y.J., Hu, R.J., and Kang, E.S.: Discussion on  
746 the present climate change from Warm2dry to Warm2wet in northwest China, *Quat. Sci.*, 23(2),  
747 152-164, 2003 (in Chinese).

748 Shepard, D.S.: Computer mapping: the SYMAP interpolation algorithm. *Spatial Statistics and*  
749 *Models*, G.L. Gaile and C.J. Willmott, Eds., D. Reidel, 133-145, 1984.

750 Sun, B., Mao, W., Feng, Y., Chang, T., Zhang, L., and Zhao, L.: Study on the change of air  
30 / 56

751 temperature, precipitation and runoff volume in the Yarkant River basin, *Arid Zone Res.*, 23(2),  
752 203-209, 2006 (in Chinese).

753 Takala, M., Luoju, K., Pulliainen, J., Derksen, C., Lemmetyinen, J., Kärnä J.-P., Koskinen, J., and  
754 Bojkov, B.: Estimating northern hemisphere snow water equivalent for climate research through  
755 assimilation of spaceborne radiometer data and ground-based measurements, *Remote*  
756 *Sens. Environ.*, 115 (12), 3517-3529, 2011.

757 Tapley, B.D., Bettadpur, S., Watkins, M., and Reigber, C.: The gravity recovery and climate  
758 experiment: mission overview and early results, *Geophys. Res. Lett.*, 31, L09607, 2004.

759 Tian, L., Yao, T., MacClune, K., White, J.W.C., Schilla, A., Vaughn, B., Vachon, R., and  
760 Ichiyonagi, K.: Stable isotopic variations in west China: a consideration of moisture sources, *J.*  
761 *Geophys. Res. Atmos.*, 112, D10112, 2007.

762 Tucker, C.J., Pinzon, J.E., Brown, M.E., Slayback, D., Pak, E.W., Mahoney, R., Vermote, E., and  
763 El Saleous, N.: An extended AVHRR 8 km NDVI data set compatible with MODIS and SPOT  
764 vegetation NDVI data, *Int. J. Remote Sens.*, 26(20), 4485-4498, 2005.

765 [von Storch, H.: Misuses of statistical analysis in climate research. In \*Analysis of Climate\*](#)  
766 [\*Variability: Applications of Statistical Techniques\*, Springer-Verlag: Berlin, 11-26, 1995.](#)

767 Wang, A. and Zeng, X.: Evaluation of multireanalysis products within site observations over the  
768 Tibetan Plateau, *J. Geophys. Res.*, 117, D05102, 2012.

769 Wang, L., Sun, L.T., Shrestha, M., Li, X.P., Liu, W.B., Zhou, J., Yang, K., Lu, H., and Chen, D.L.:  
770 Improving snow process modeling with satellite-based estimation of  
771 near-surface-air-temperature lapse rate, *J. Geophys. Res. Atmos.*, 121, 12005-12030, 2016.

772 Xia, Y., Mitchell, K., Ek, M., Cosgrove, B., Sheffield, J., Luo, L., Alonge, C., Wei, H., Meng, J.,  
773 Livneh, B., and Duang, Q.: Continental-scale water and energy flux analysis and validation for  
774 North American Land Data Assimilation System project phase 2 (NLDAS-2): 2. Validation of  
775 model-simulated streamflow, *J. Geophys. Res. Atmos.*, 117(D3), D03110, 2012.

776 [Xiang, L., Wang, H., Steffen, H., Wu, P., Jia, L., Jiang, L., and Shen, Q.: Groundwater storage](#)  
777 [changes in the Tibetan Plateau and adjacent areas revealed from GRACE satellite gravity data,](#)  
778 [\*Earth Planet. Sci. Lett.\*, 449, 228-239, 2016.](#)

779 Xu, L.: The land surface water and energy budgets over the Tibetan Plateau, Available from  
780 Nature Precedings < <http://hdl.handle.net/10101/npre.2011.5587.1>>, 2011.

781 Xue, B.L., Wang, L., Yang, K., Tian, L., Qin, J., Chen, Y., Zhao, L., Ma, Y., Koike, T., Hu, Z., and  
782 Li, X.P.: Modeling the land surface water and energy cycle of a mesoscale watershed in the  
783 central Tibetan Plateau with a distributed hydrological model, *J. Geophys. Res. Atmos.*, 118,  
784 8857-8868, 2013.

785 Yao, Z., Duan, R., and Liu, Z.: Changes in precipitation and air temperature and its impacts on  
786 runoff in the Nuijiang River basins. *Resour. Sci.* 34(2), 202-210, 2012 (in Chinese)

787 Yang, K., Qin, J., Zhao, L., Chen, Y.Y., Tang, W.J., Han, M.L., Lazhu, Chen, Z.Q., Lv, N., Ding,  
788 B.H., Wu, H., and Lin, C.G.: A multi-scale soil moisture and freeze-thaw monitoring network  
789 on the third pole, *Bull. Am. Meteorol. Soc.*, 94,1907-1916, 2013.

790 Yang, K., Wu, H., Qin, J., Lin, C.G., Tang, W.J., and Chen, Y.Y.: Recent climate changes over the  
791 Tibetan Plateau and their impacts on energy and water cycle: a review, *Glob. Planet Change*,  
792 112, 79-91, 2014.

793 Yao, T.D., Thompson, L., Yang, W., Yu, W.S., Gao, Y., Guo, X.J., Yang, X.X., Duan, K.Q., Zhao,  
794 H.B., Xu, B.Q., Pu, J.C., Lu, A.X., Xiang, Y., Kattel, D.B., and Joswiak, D.: Different glacier  
795 status with atmospheric circulations in Tibetan Plateau and surroundings, *Nat. Clim. Change*, 2,  
796 1-5, 2012.

797 [Yao, Y.J., Zhao, S.H., Zhang, Y.H., Jia, K., and Liu, M.: Spatial and decadal variations in potential](#)  
798 [evapotranspiration of China based on reanalysis datasets during 1982-2010. \*Atmosphere\*, 5,](#)  
799 [737-754, 2014.](#)

800 Yin, G., Hu, Z.Y., Chen, X., and Tiyip, T.: Vegetation dynamics and its response to climate change  
801 in Central Asia, *J. Arid Land*, 8, 375, 2016.

802 Yu, J., Zhang, G., Yao, T., Xie, H., Zhang, H., Ke, C., and Yao, R.: Developing daily cloud-free  
803 snow composite products from MODIS Terra-Aqua and IMS for the Tibetan Plateau, *IEEE*  
804 *Trans. Geosci. Remote Sens.*, 54(4), 2171-2180, 2015.

805 [Yue, S., Pilon, P., Phinney, B., Cavadias, G.: The influence of autocorrelation on the ability to](#)  
806 [detect trend in hydrological series. \*Hydrol. Process.\*, 16\(9\), 1807-1829, 2002.](#)

807 Zhang, D., Liu, X., Zhang, Q., Liang, K., and Liu, C.: Investigation of factors affecting  
808 inter-annual variability of evapotranspiration and streamflow under different climate conditions.



809 J. Hydrol., doi:10.1016/j.jhydrol.2016.10.047, 2016.

810 Zhang, G., Xie, H., Yao, T., Liang, T., and Kang, S.: Snow cover dynamics of four lake basins  
811 over Tibetan Plateau using time series MODIS data (2001-2100), *Water Resour. Res.*, 48(10),  
812 W10529, 2012.

813 Zhang, K., Kimball, J.S., Nemani, R.R., and Running, S.W.: A continuous satellite-derived global  
814 record of land surface evapotranspiration from 1983 to 2006, *Water Resour. Res.*, 46(9),  
815 W09522, 2010.

816 Zhang, L., Su, F., Yang, D., Hao, Z., and Tong, K.: Discharge regime and simulation for the  
817 upstream of major rivers over Tibetan Plateau, *J. Geophys. Res. Atmos.*, 118(15), 8500-8518,  
818 2013.

819 [Zhang, Q., Li, J., Singh, V., and Xu, C.: Copula-based spatial-temporal patterns of precipitation  
820 extremes in China, \*Int. J. Climatol.\*, 33, 1140-1152, 2013.](#)

821 Zhang, X., Tang, Q., Pan, M., and Tang, Y.: A long-term land surface hydrologic fluxes and states  
822 dataset for China, *J. Hydrometeorol.*, 15, 2067-2084, 2014.

823 Zhang, Y., Peña-Arancibia, J.L., McVicar, T.R., Chiew, F.H.S., Vaze, J., Liu, C.M., Lu, X.J.,  
824 Zheng, H.X., Wang, Y.P., Liu, Y.Y., Miralles, D.G., and Pan, M.: Multi-decadal trends in global  
825 terrestrial evapotranspiration and its components, *Scientific Reports*, 6, 19124, 2016.

826 Zhang, Y., Liu, C., Tang, Y., and Yang, Y.: Trend in pan evaporation and reference and actual  
827 evapotranspiration across the Tibetan Plateau, *J. Geophys. Res.*, 112, D12110, 2007.

828 Zhou, C., Jia, S., Yan, H., and Yang, G.: Changing trend of water resources in Qinghai Province  
829 from 1956 to 2000, *J. Glaciol. Geocryol.*, 27(3), 432-437, 2005 (in Chinese).

830 Zhou, J., Wang, L., Zhang, Y.S., Guo, Y.H., Li, X.P., and Liu, W.B.: Exploring the water storage  
831 changes in the largest lake (Selin Co) over the Tibetan Plateau during 2003-2012 from a  
832 basin-wide hydrological modeling, *Water Resour. Res.*, 51, 8060-8086, 2015.

833 Zhou, S.Q., Kang, S., Chen, F., and Joswiak, D.R.: Water balance observations reveal significant  
834 subsurface water seepage from Lake Nam Co., south-central Tibetan Plateau, *J. Hydrol.*, 491,  
835 89-99, 2013.

836 Zhou, S.Q., Wang, Z., and Joswiak, D.R.: From precipitation to runoff: stable isotopic fractionation  
837 effect of glacier melting on a catchment scale, *Hydrol. Process.*, 28(8), 3341-3349, 2014.

838 Zhu, Y., Chen, J., Chen, G.: Runoff variation and its impacting factors in the headwaters of the

839 Yangtze River in recent 32 years, J. Yangtze River Sci. Res. Inst., 28(6), 1-4, 2011 (in Chinese).

840 **Table 1:** Main features of the 18 used TP river basins. GA% and SC% represent the percentages of multiyear-mean glacier cover and snow cover in each basin.  
841 The glacier and snow cover data are extracted, respectively, from the Second Glacier Inventory Dataset of China and the daily TP snow cover dataset  
842 (2005-2013)  
843

No.	Station	Altitude (m)	River name	Drainage area (km <sup>2</sup> )	Multiyear-mean (1982-2011) and basin-averaged parameters						
					Q (mm/yr)	Prec. (mm/yr)	Temp.(°C/yr)	NDVI	LAI	GA%	SC%
01	Kulukelangan	2000	Yerqiang	32880.00	158.60	128.34	-5.68	0.05	0.03	10.97	35.03
02	Tongguziluoke	1650	Yulongkashi	14575.00	151.56	134.04	-4.07	0.06	0.04	23.27	35.95
03	Numaitilangan	1880	Keliya	7358.00	103.18	137.14	-4.78	0.06	0.03	10.86	29.16
04	Zelingou	4282	Bayin	5544.00	41.42	340.68	-4.98	0.13	0.09	0.09	21.22
05	Gadatan	3823	Yellow	7893.00	200.95	566.01	-4.60	0.34	0.54	0.13	14.94
06	Xining	3225	Yellow	9022.00	99.90	503.74	0.97	0.36	0.70	0.00	10.06
07	Tongren	3697	Yellow	2832.00	149.36	533.25	-1.37	0.39	0.83	0.00	9.42
08	Tainaihai	2632	Yellow	121972.00	159.48	540.32	-2.40	0.34	0.72	0.09	15.89
09	Huangheyang	4491	Yellow	20930.00	31.18	386.42	-4.81	0.23	0.61	0.00	17.25
10	Jimai	4450	Yellow	45015.00	85.50	441.48	-4.16	0.26	0.52	0.00	20.05
11	Yajiang	2599	Yalong	67514.00	237.66	717.05	-0.23	0.43	0.80	0.15	18.36
12	Zhimenda	3540	Yangtze	137704.00	96.23	405.66	-4.83	0.20	0.26	0.96	17.87
13	Jiaoyuqiao	3000	Salween	72844.00	364.26	620.88	-1.89	0.29	0.44	2.02	23.73
14	Pangduo	5015	Brahmaputra	16459.00	348.31	544.59	-1.53	0.27	0.33	1.66	23.33
15	Tangjia	4982	Brahmaputra	20143.00	350.61	555.17	-1.89	0.27	0.34	1.39	21.83
16	Gongbujiangda	4927	Brahmaputra	6417.00	586.96	692.06	-4.24	0.27	0.36	4.12	25.99
17	Nuxia	2910	Brahmaputra	191235.00	307.38	401.35	-0.73	0.22	0.25	1.90	13.50
18	Yangcun	3600	Brahmaputra	152701.00	163.25	349.91	-0.87	0.19	0.18	1.28	10.52

844  
845

846 **Table 2:** Overview of multi-source datasets applied in this study

847

Data category	Data source	Spatial resolution	Temporal resolution	Available period used	Reference
Runoff (Q)	Observed, National Hydrology Almanac of China	—	Daily	1982-2011	—
	VIC_IGSNRR simulated	0.25°	Daily	1982-2011	Zhang et al. (2014)
Precipitation (P)	Observed, CMA	0.5°	Monthly	1982-2011	—
	TRMM 3B43 V7	0.25°	Monthly	2000-2011	Huffman et al. (2012)
	IGSNRR forcing	0.25°	Daily	1982-2011	Zhang et al. (2014)
Temperature (Temp.)	Observed, CMA	0.5°	Monthly	2000-2011	—
Terrestrial storage change (ΔS)	GRACE-CSR	Approx.300-400 km	Monthly	2002-2011	Tapley et al. (2004)
	GRACE-GFZ	Approx.300-400 km	Monthly	2002-2011	Tapley et al. (2004)
	GRACE-JPL	Approx.300-400 km	Monthly	2002-2011	Tapley et al. (2004)
Potential evaporation (PET)	CRU	0.5°	Monthly	1982-2011	Harris et al. (2013)
Actual evaporation (ET)	MTE_E	0.5°	Monthly	1982-2011	Jung et al. (2010)
	VIC_E	0.25°	Daily	1982-2011	Zhang et al. (2014)
	GLEAM_E	0.25°	Daily	1982-2011	Miralles et al. (2011)
	PML_E	0.5°	Monthly	1982-2011	Zhang Y et al. (2016)
	Zhang_E	8 km	Monthly	1983-2006	Zhang et al. (2010)
	GNoah_E	1.0°	3 hourly	1982-2011	Rui (2011)
NDVI	GIMMS NDVI dataset	8 km	15 daily	1982-2011	Tucker et al. (2005)
LAI	GLASS LAI Product	0.05°	8 daily	1982-2011	Liang and Xiao (2012)
Snow Cover	TP Snow composite Products	500 m	Daily	2005-2013	Zhang et al. (2012)
SWE	VIC_IGSNRR simulated	0.25°	Daily	1982-2011	Zhang et al. (2014)
	GlobSnow-2 Product	25 km	Daily	1982-2011	Takala et al. (2011)

848

849 **Table 3:** Contribution of glacier-melt to discharge in eighteen basins (“—” shows no glacier influences, “—\*” shows the percentage is empirically estimated  
850 | through the relation between lacier area ratio and glacier melt for basins in which the glacier melt contribution has been reported in [existing studies the literatures](#))  
851

Basin	Contributions of glacier-melt to discharge (%)	Reference
Kulukelangan	62.73	Mansur and Ajnisa (2005)
Tongguziluoke	64.90	Liu J et al. (2016)
Numaitilangan	71	Chen (1988)
Zelingou	—	—
Gadatan	—	—
Xining	—	—
Tongren	—	—
Tainaihai	0.80	Zhang et al. (2013)
Huangheyuan	—	—
Jimai	—	—
Yajiang	1.40	—*
Zhimenda	6.50	Zhang et al. (2013)
Jiaoyuqiao	4.80	Zhang et al. (2013)
Nuxia	11.60	Zhang et al. (2013)
Pangduo	10.13	—*
Tangjia	8.49	—*
Gongbujiangda	25.15	—*
Yangcun	7.81	—*

852  
853  
854

855 **Table 4:** Nonparametric trends for different ET estimates during the period 1982-2006 detected by modified Mann-Kendall test, the bold number showed the  
 856 detected trend is statistically significant at the 0.05 level

857	Basin	$ET_{wb}$	ET <sub>wb</sub>	GLEAM_E	VIC_E	Zhang_E	PML_E	MET_E	GNoah_E
859	Kulukelangan	<b>-0.09</b>		0.09	<b>0.18</b>	–	0.03	-0.01	0.07
	Tongguziluo	-0.02		0.10	<b>0.13</b>	–	0.03	<b>-0.08</b>	0.19
860	Numaitilangan	0.04		<b>0.10</b>	0.14	–	0.14	<b>-0.10</b>	0.22
	Zelingou	<b>0.13</b>		<b>0.23</b>	0.11	<b>0.09</b>	0.04	<b>0.06</b>	0.02
861	Gadatan	-0.09		0.25	0.070	-0.10	-0.01	<b>0.06</b>	-0.07
	Xining	-0.06		<b>0.54</b>	0.01	-0.08	0.01	0.02	-0.06
862	Tongren	-0.06		<b>0.34</b>	-0.15	<b>-0.17</b>	0.07	0.02	0.13
	Tainaihai	0.06		<b>0.28</b>	-0.03	<b>-0.11</b>	0.04	<b>0.05</b>	0.04
863	Huangheyang	0.08		<b>0.19</b>	-0.01	<b>-0.10</b>	<b>0.08</b>	<b>0.05</b>	<b>0.10</b>
	Jimai	-0.07		<b>0.23</b>	-0.01	-0.08	0.03	<b>0.05</b>	0.10
864	Yajiang	0.17		<b>0.26</b>	<b>0.06</b>	<b>-0.21</b>	-0.01	0.03	-0.02
	Zhimenda	0.11		<b>0.28</b>	0.10	0.01	0.07	<b>0.04</b>	0.07
865	Jiaoyuqiao	<b>0.18</b>		<b>0.28</b>	0.10	<b>-0.11</b>	0.05	<b>0.05</b>	0.07
	Nuxia	<b>-0.09</b>		<b>0.25</b>	0.09	<b>-0.10</b>	<b>0.12</b>	<b>0.04</b>	0.10
866	Pangduo	0.05		<b>0.28</b>	<b>0.17</b>	<b>-0.07</b>	0.07	<b>0.07</b>	<b>0.11</b>
	Tangjia	0.09		<b>0.26</b>	<b>0.17</b>	<b>-0.09</b>	<b>0.20</b>	<b>0.06</b>	<b>0.12</b>
867	Gongbujiangda	-0.26		0.12	0.13	<b>-0.16</b>	<b>0.19</b>	0.01	<b>0.15</b>
	Yangcun	0.03		<b>0.28</b>	0.08	<b>-0.06</b>	0.10	0.04	0.09

868

869

870 **Figure captions:**

871 **Figure 1.** Map of river basins and hydrological gauging stations (green dots) over the  
872 Tibetan Plateau (TP) used in this study. The grey shading shows the topography of TP  
873 in meters above the sea level and the blue shading exhibits the glaciers distribution in  
874 TP extracted from the Second Glacier Inventory Dataset of China.

875 **Figure 2.** Comparison of VIC\_IGSNRR simulated and observed monthly runoff for  
876 Tangnaihai and Panduo stations (a and b) as well as (c) basin-averaged monthly  
877 TRMM, CMA gridded and IGSNRR forcing precipitations for the smallest basin  
878 (Tongren station) over the period 1982-2011. (d) ~~shows~~Shows the comparison of  
879 TRMM (blue) and IGSNRR forcing (red) precipitations against CMA gridded  
880 precipitation for 18 river basins over TP during the period 2000-2011.

881 **Figure 3.** Comparison of different ET products against the calculated ET through the  
882 water balance method ( $ET_{wb}$ ) for 18 TP basins. The boxplot of annual estimates  
883 of different ET products for 18 TP basins are shown in (a) while the correlation  
884 coefficients and root-mean-square-errors (RMSEs, mm/month) for each ET product  
885 relatively to  $ET_{wb}$  are exhibited in (b).

886 **Figure 4.** General water and energy status (a. the perspective of Budyko framework)  
887 and their relationships with glacier (b) and vegetation (c and d) for eighteen TP river  
888 basins (1983-2006). The ET used in this figure is calculated from the bias-corrected  
889 water balance method.

890 **Figure 5.** Seasonal cycles (1982-2011) of water budget components in westerlies-  
891 dominated (column 1), East Asian monsoon-dominated (columns 2-4) and Indian  
892 monsoon-dominated (columns 5-6) TP basins.

893 **Figure 6.** Seasonal cycles (1982-2011) of air temperature and vegetation parameters  
894 in westerlies-dominated (column 1), East Asian monsoon-dominated (columns 2-4)  
895 and Indian monsoon-dominated (columns 5-6) TP basins.

896 **Figure 7.** Seasonal cycles (1982-2011) of snow cover and snow water equivalent  
897 (SWE) in westerlies-dominated (column 1), East Asian monsoon-dominated (columns  
898 2-4) and Indian monsoon-dominated (columns 5-6) TP basins. The snow cover was

899 extracted from cloud free snow composite product during the period 2005-2013. It  
900 should also be noted that the GlobSnow data are not available for some basins.

901 **Figure 8.** Sen's slopes of water budget components and vegetation parameters in  
902 westerlies-dominated TP basins during the period of 1982-2011. The double red stars  
903 showed that the trend was statistically significant at the 0.05 level.

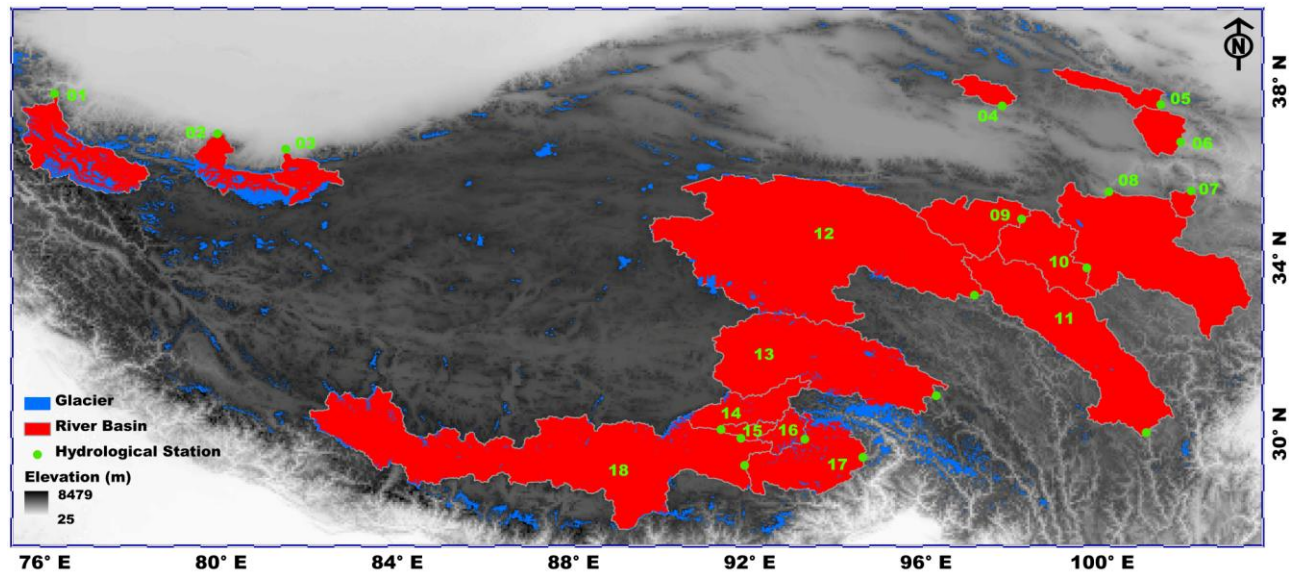
904 **Figure 9.** Linear and non-parametric trends of westerly, Indian monsoon and East  
905 Asian summer monsoon during the period 1982-2011 revealed prospectively by the  
906 Asian Zonal Circulation Index, Indian Ocean Dipole Mode Index and East Asian  
907 Summer Monsoon Index.

908 **Figure 10.** Similar to Figure 8 but for East Asian monsoon-dominated TP basins. It  
909 should be noted that the GlobSnow data are not available for some basins. The double  
910 red stars showed that the trend was statistically significant at the 0.05 level.

911 **Figure 11.** Similar to Figure 8 but for Indian monsoon-dominated TP basins. It should  
912 be noted that the GlobSnow data are not available for some basins. The double red  
913 stars showed that the trend was statistically significant at the 0.05 level.

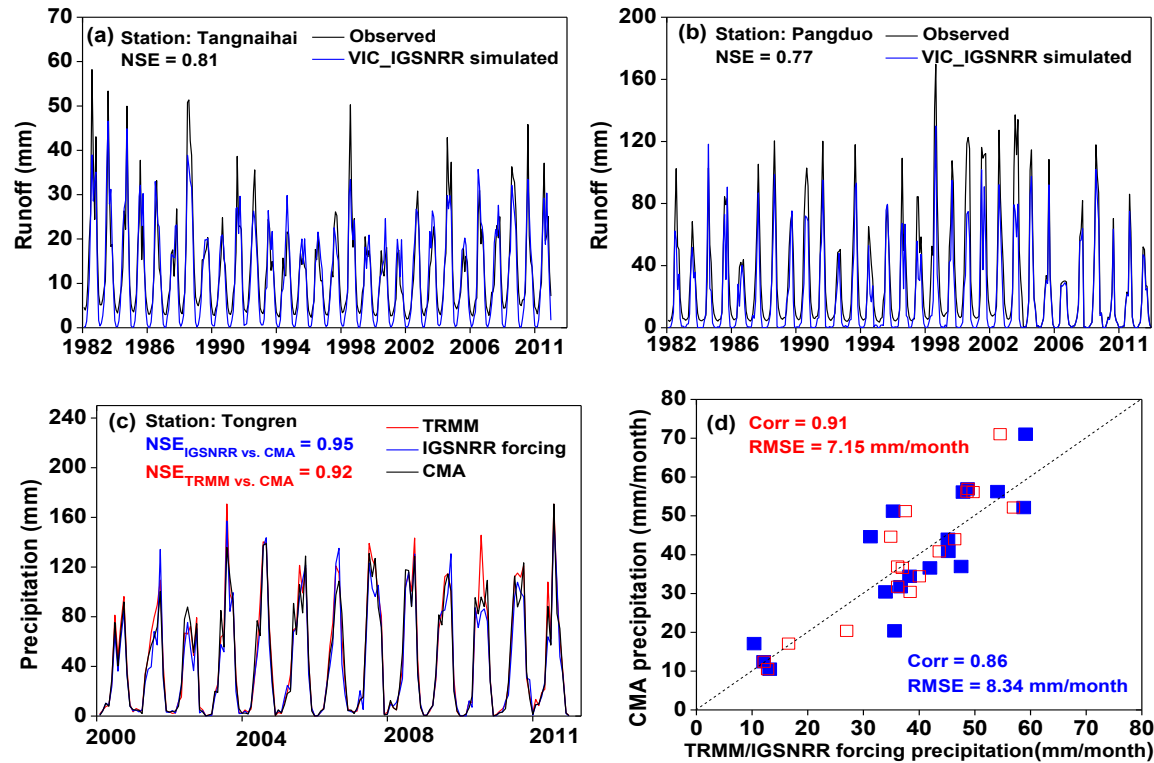


914 **Figure 1.** Map of river basins and hydrological gauging stations (green dots) over the Tibetan Plateau (TP) used in this study. The grey shading shows the  
915 topography of TP in meters above the sea level and the blue shading exhibits the glaciers distribution in TP extracted from the Second Glacier Inventory Dataset of  
916 China.



917  
918

919 **Figure 2.** Comparison of VIC\_IGSNRR simulated and observed monthly runoff for Tangnaihai and Panduo stations (a and b) as well as (c) basin-averaged  
 920 monthly TRMM, CMA gridded and IGSNRR forcing precipitations for the smallest basin (Tongren station) over the period 1982-2011. (d) shows the comparison of  
 921 TRMM (blue) and IGSNRR forcing (red) precipitations against CMA gridded precipitation for 18 river basins over TP during the period 2000-2011.

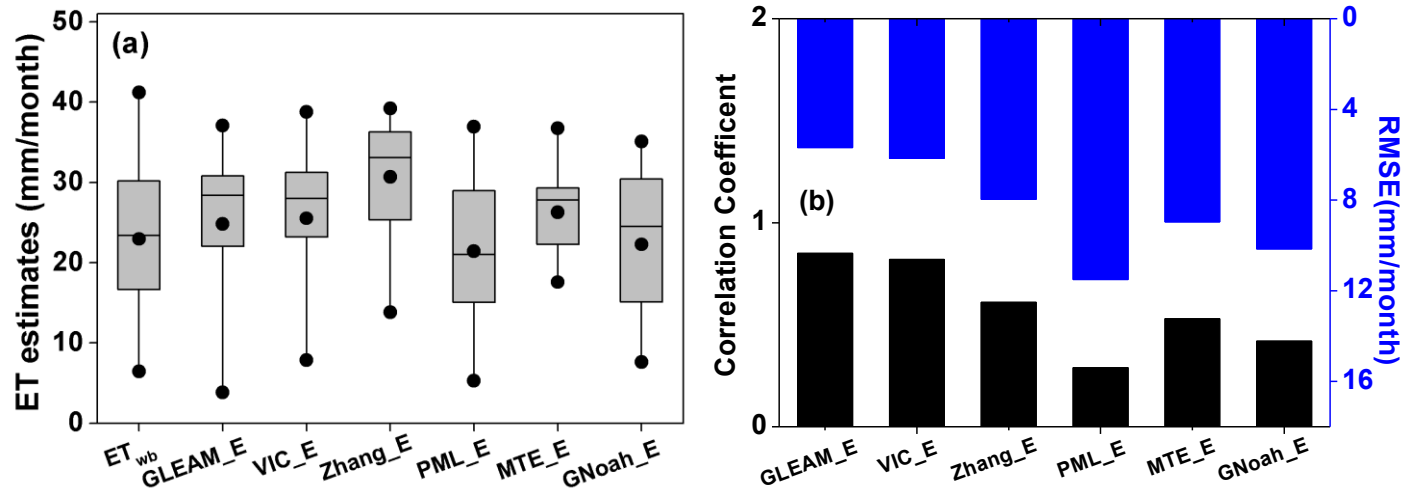


922

923  
 924

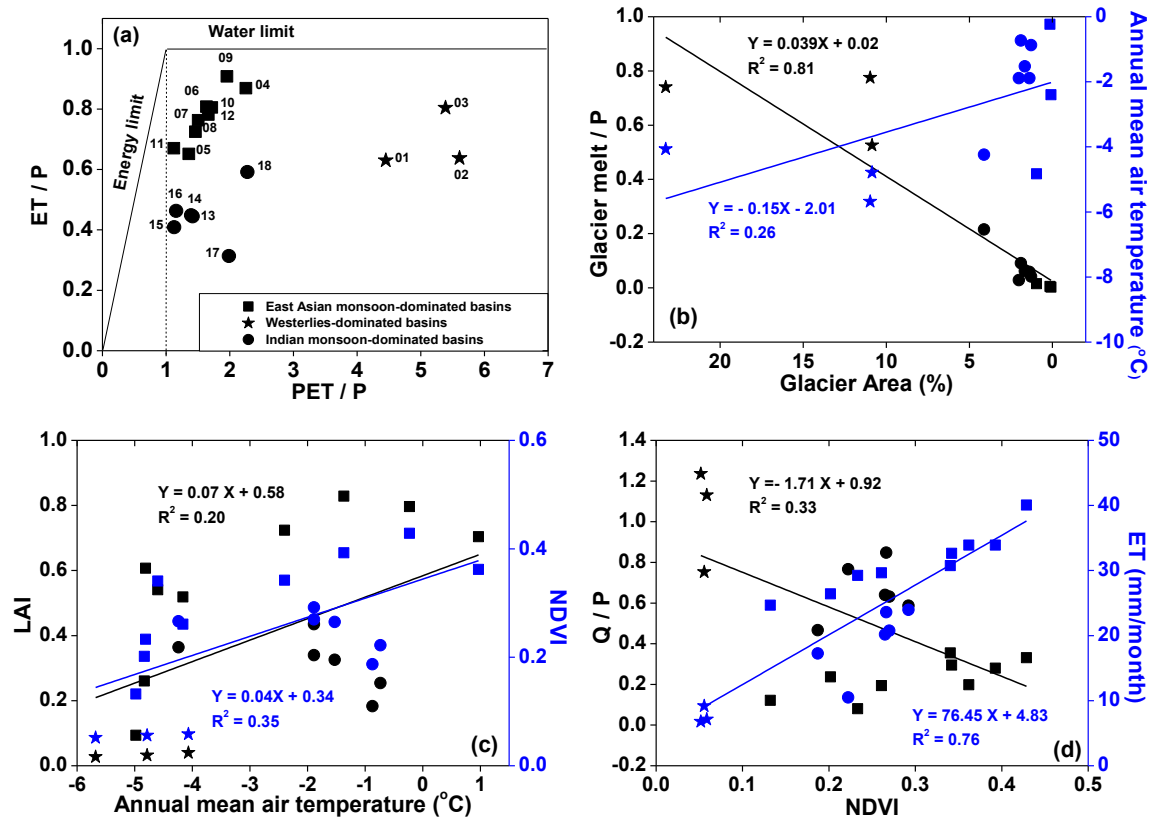
925 | **Figure 3.** Comparison of different ET products against the calculated ET through the water balance ( $ET_{wb}$ ) for 18 river basins over the Tibetan Plateau. The  
 926 | boxplot of annual estimates of different ET products for 18 TP basins are shown in (a) while the correlation coefficients and root-mean-square-errors (RMSEs,  
 927 | mm/month) for each ET product relatively to  $ET_{wb}$  are exhibited in (b).

带格式的: 字体: 五号  
 带格式的: 字体: 五号



928  
 929

930 **Figure 4.** General water and energy status (a. the perspective of Budyko framework) and their relationships with glacier (b) and vegetation (c and d) for eighteen  
 931 TP river basins (1983-2006). The ET used in this figure is calculated from the bias-corrected water balance method.

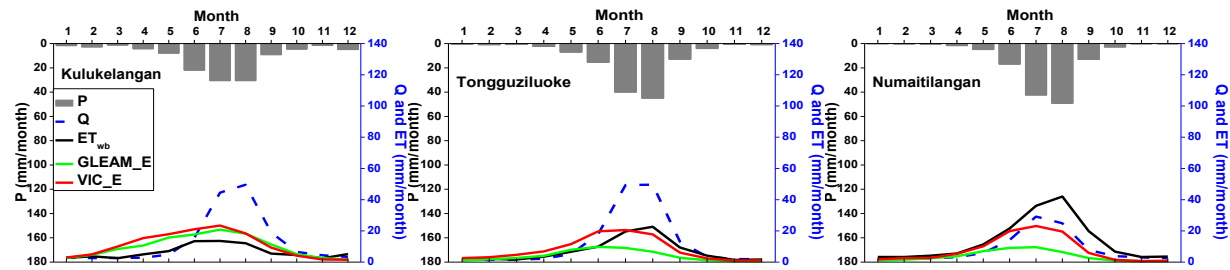


932

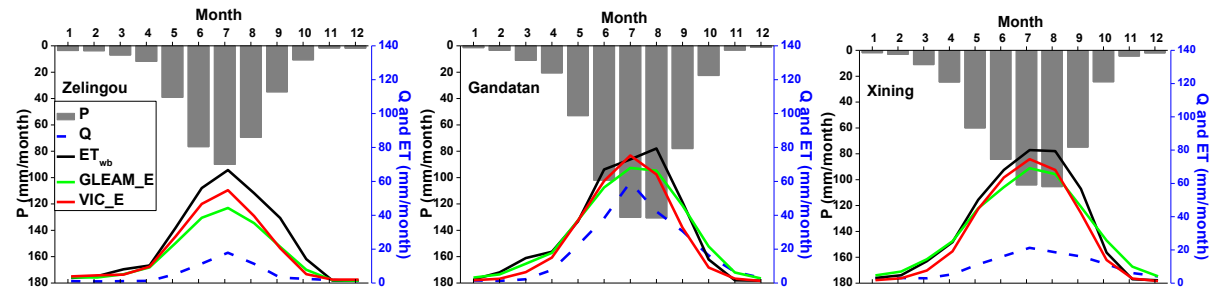
933

934 **Figure 5.** Seasonal cycles (1982–2011) of water budget components in westerlies-dominated (column 1), East Asian monsoon-dominated (columns 2–4) and Indian  
 935 monsoon-dominated (columns 5–6) TP basins.

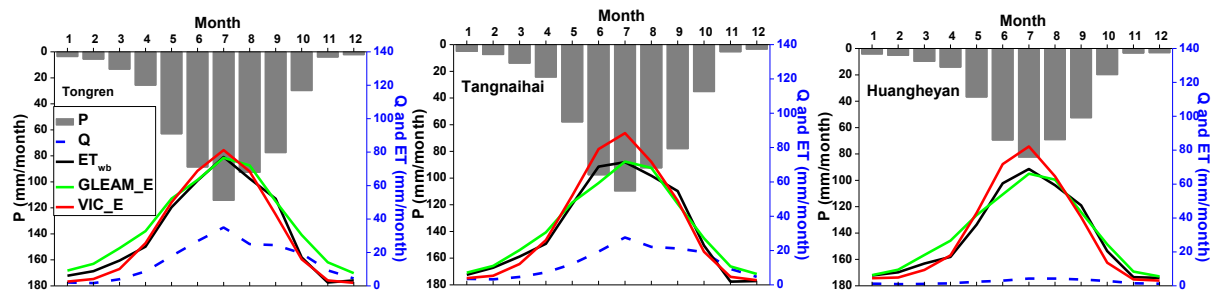
936



937

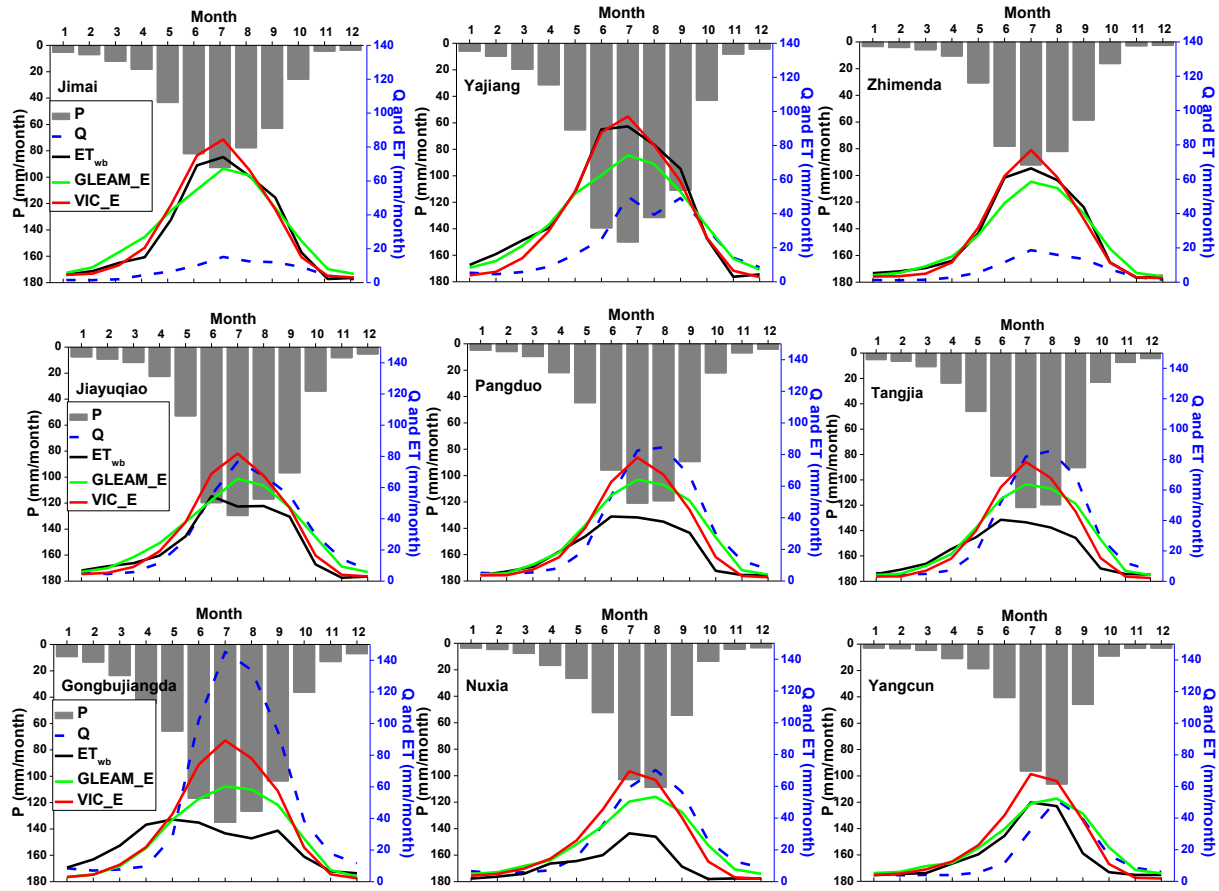


938



939

Figure 5: (continued)

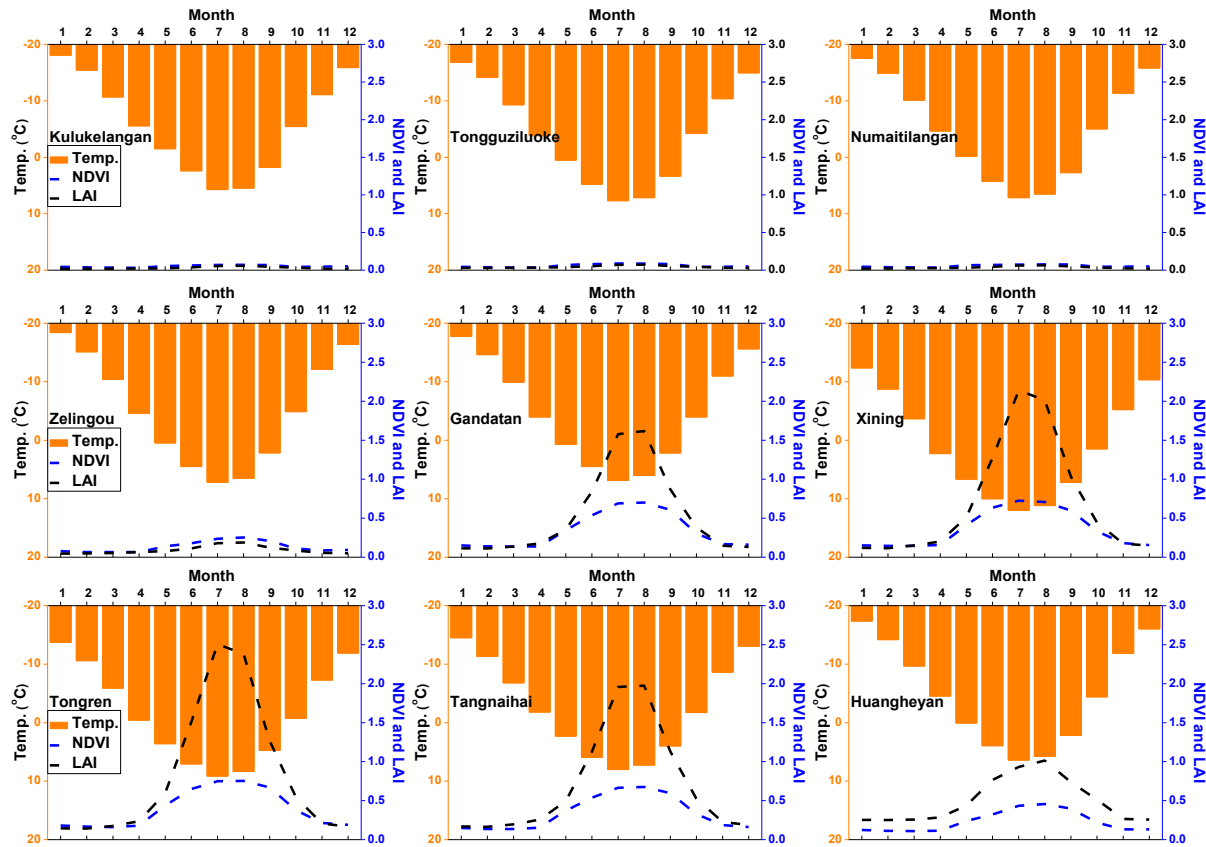


940

941

942

943 **Figure 6.** Seasonal cycles (1982-2011) of air temperature and vegetation parameters in westerlies-dominated (column 1), East Asian monsoon-dominated (columns  
 944 2-4) and Indian monsoon-dominated (columns 5-6) TP basins.



945

946

947

948

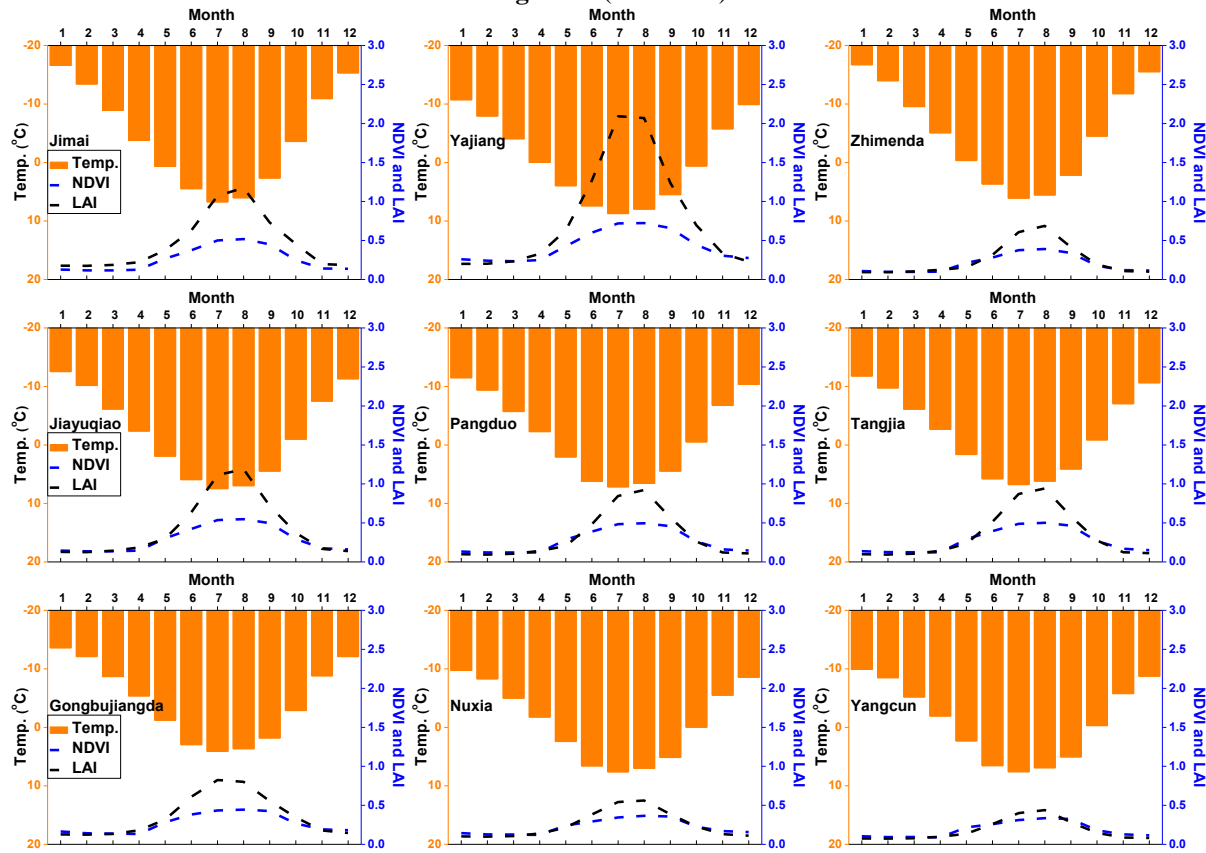
949

950

951

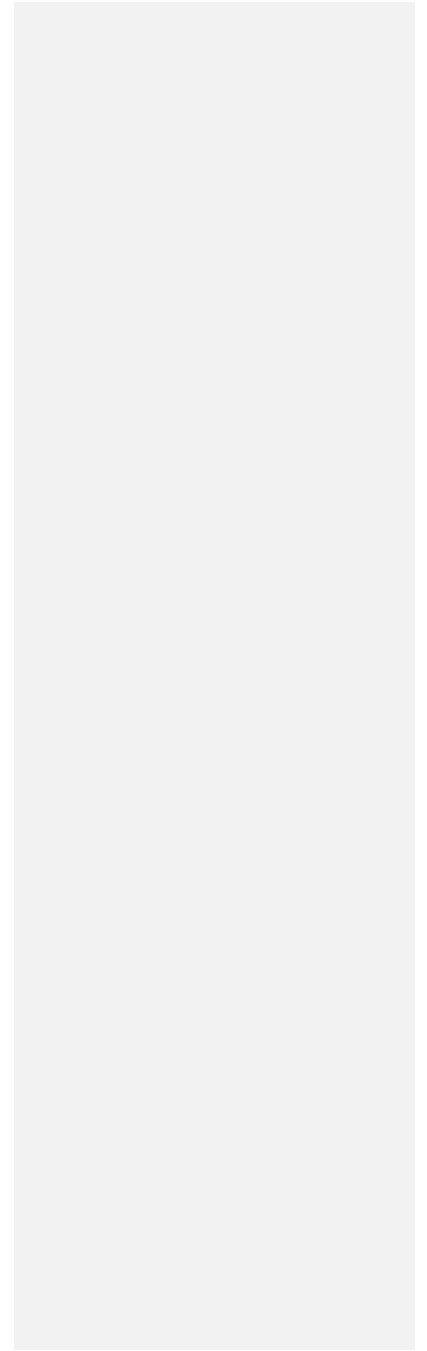
952

Figure 6: (continued)

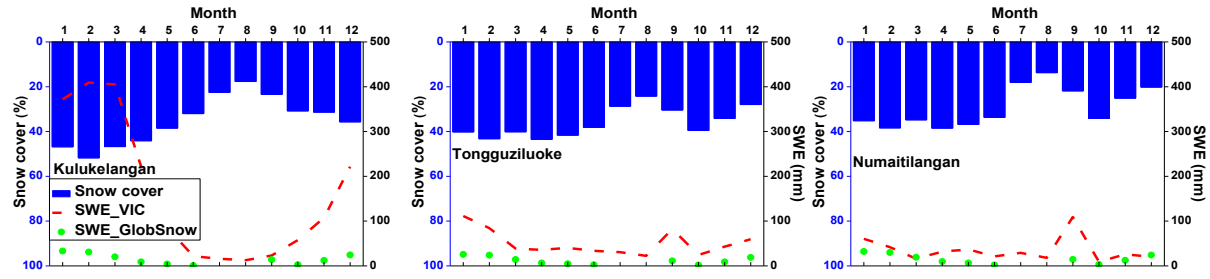




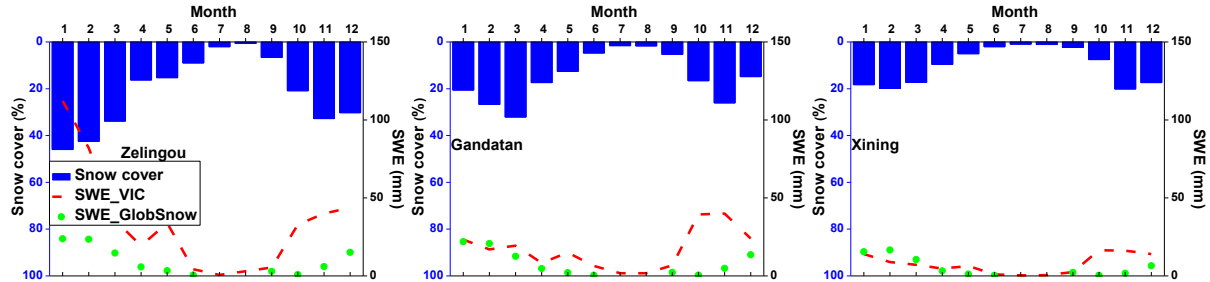
953 **Figure 7.** Seasonal cycles (1982-2011) of snow cover and snow water equivalent (SWE) in westerlies-dominated (column 1), East Asian monsoon- dominated  
954 (columns 2-4) and Indian monsoon-dominated (columns 5-6) TP basins. The snow cover was extracted from cloud free snow composite product during the period  
955 2005-2013. It should also be noted that the GlobSnow data are not available for some basins.  
956



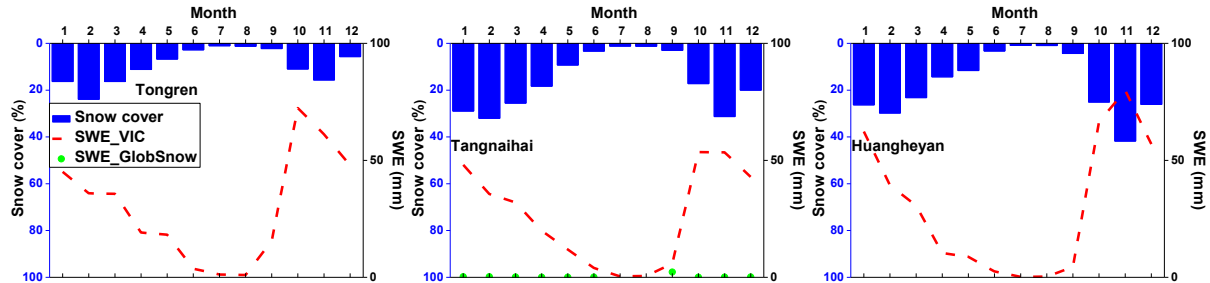
957



958



959

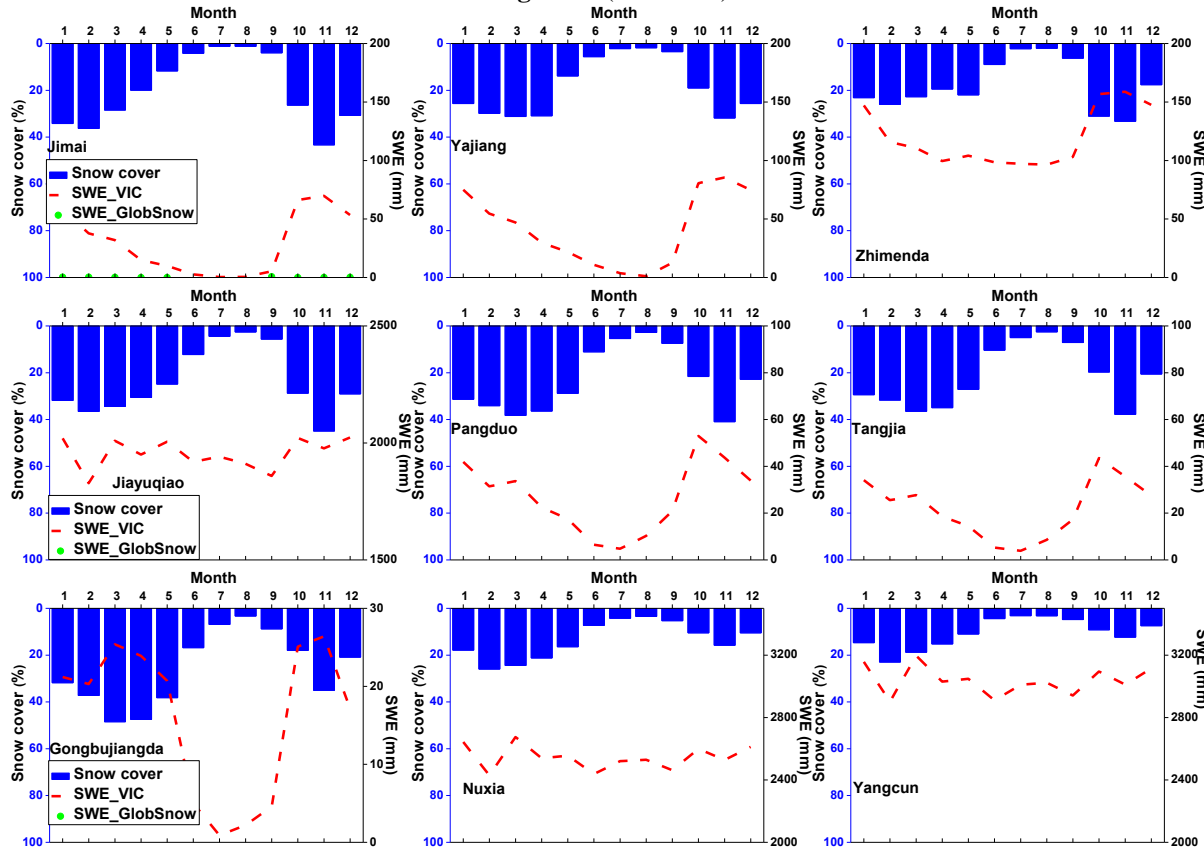


960

961

962

Figure 7: (continued)



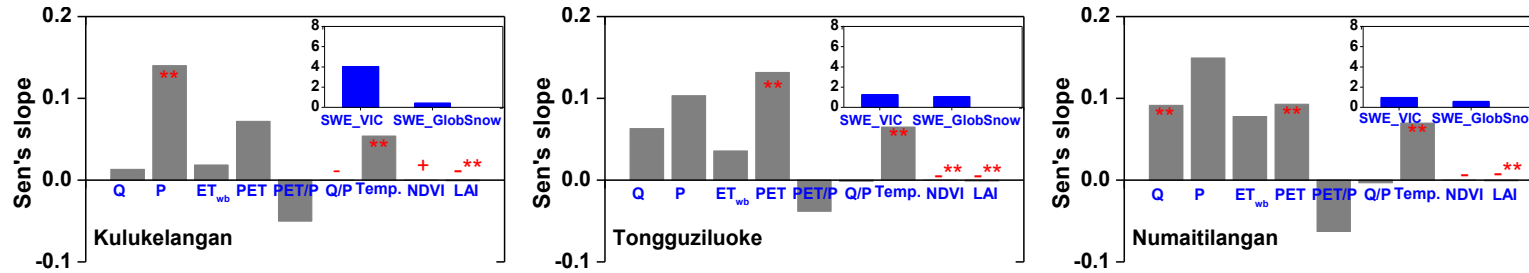
963

964

965

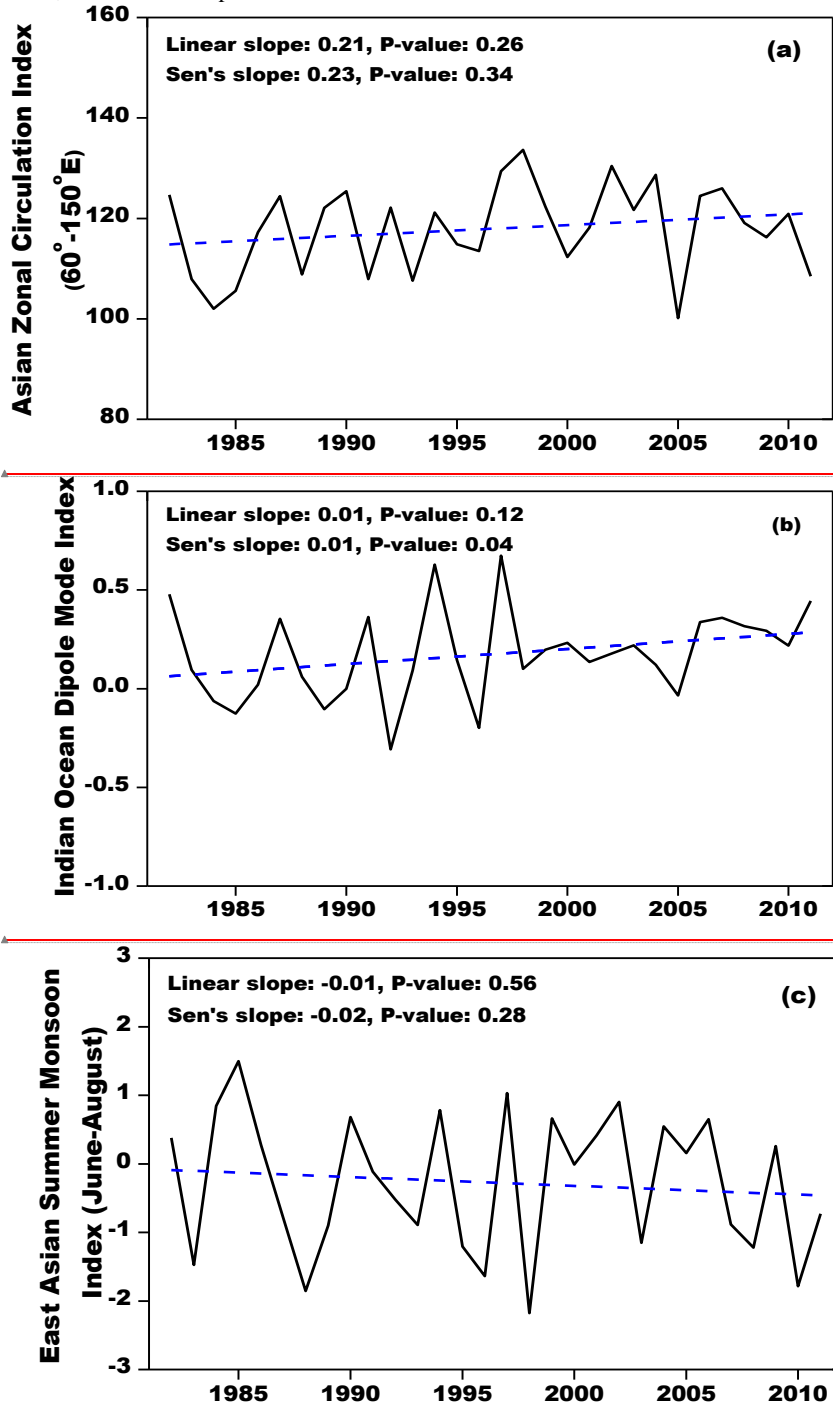
966

967 **Figure 8.** Sen's slopes of water budget components and vegetation parameters in westerlies-dominated TP basins during the period of 1982-2011. The double red  
 968 stars showed that the trend was statistically significant at the 0.05 level.



969  
 970

971 | **Figure 9.** Linear and non-parametric trends of westerly, Indian monsoon and East Asian summer  
 972 monsoon during the period 1982-2011 revealed prospectively by the Asian Zonal Circulation  
 973 Index, Indian Ocean Dipole Mode Index and East Asian Summer Monsoon Index.



域代码已更改

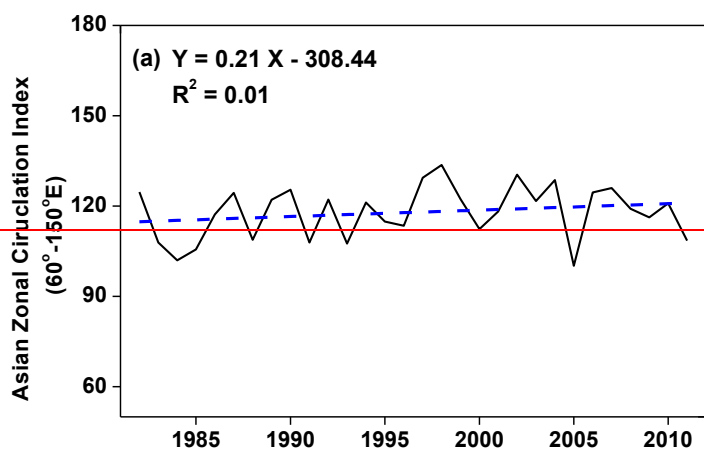
域代码已更改

带格式的: 左  
 域代码已更改

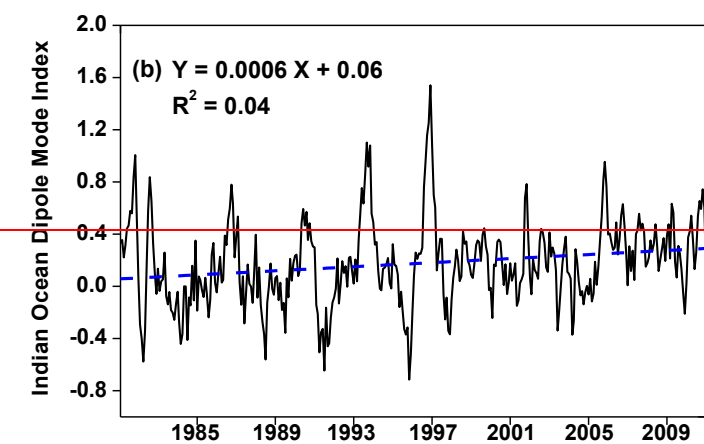
974

975

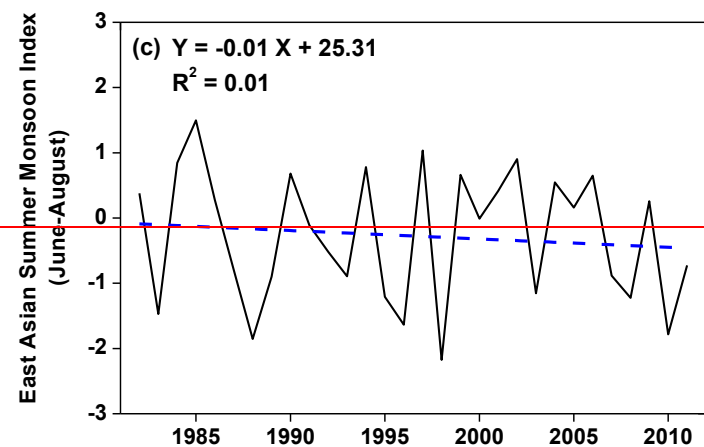
976



977



978



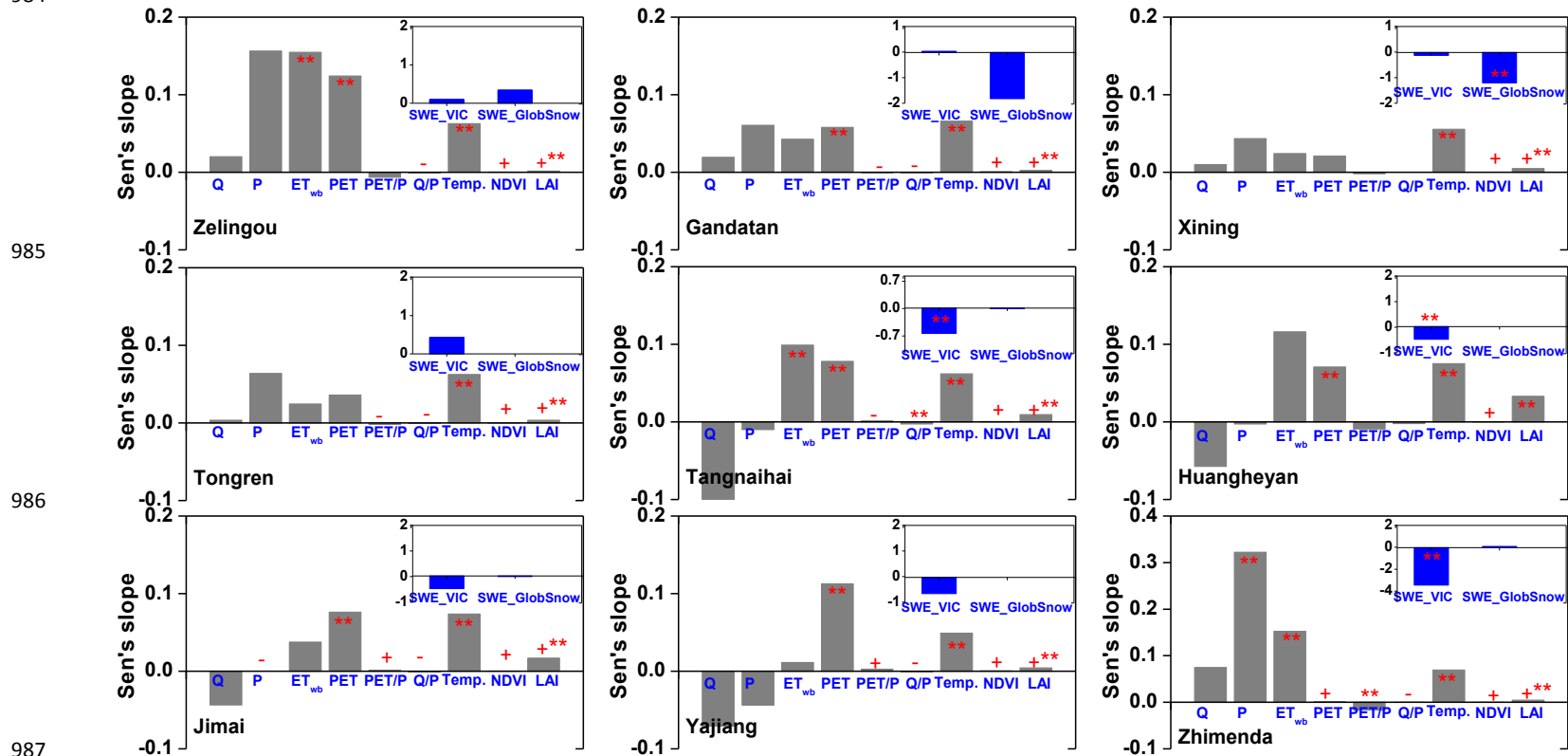
979

980

981

带格式的：两端对齐

982 **Figure 10.** Similar to Figure 8 but for East Asian monsoon-dominated TP basins. It should be noted that the GlobSnow data are not available for some basins. The  
 983 double red stars showed that the trend was statistically significant at the 0.05 level.  
 984



990 **Figure 11.** Similar to Figure 8 but for Indian monsoon-dominated TP basins. It should be noted that the GlobSnow data are not available for some basins. The  
 991 double red stars showed that the trend was statistically significant at the 0.05 level.  
 992

